ELSEVIER

Marine Geology 224 (2005) 57–82

MARINE GEOLOGY
INTERNATIONAL JOURNAL OF MARINE GEOLOGY, GEOCHEMISTRY AND GEOPHYSICS

www.elsevier.com/locate/margeo

Palaeoclimatology and palaeohydrography of the glacial stages on Celtic and Armorican margins over the last 360 000 yrs

M. Mojtahid [a,1], F. Eynaud [a,*], S. Zaragosi [a], J. Scourse [b], J.-F. Bourillet [c], T. Garlan [d]

[a] *Département Géologie et Océanographie, UMR-CNRS "EPOC" 5805, Université Bordeaux I, Avenue des Facultés, F-33405 Talence, France*
[b] *School of Ocean Sciences, University of Wales (Bangor), Menai Bridge, Anglesey, LL59 5EY, UK*
[c] *IFREMER, Département Géosciences Marines, Laboratoire Environnements Sédimentaires, BP 70- 29280 Plouzané, France*
[d] *EPSHOM, 13, rue du Chatellier- BP 30316- 29603 BREST Cedex, France*

Received 14 February 2005; received in revised form 19 July 2005; accepted 21 July 2005

Abstract

Core MD03-2692 was retrieved in a water-depth of 4064 m on the Celtic margin (Bay of Biscay) during the SEDICAR cruise onboard the *RV Marion Dufresne II*. It covers the last 360 ka in a total length of 39 m. Multidisciplinary analyses have been applied to this sequence with the aim of studying the palaeoclimatic and palaeoenvironmental signals of the last few climatic cycles. The analyses undertaken include: (1) non-destructive logging with: physical properties (magnetic susceptibility, sediment colour), X-ray radiography and measurement of the major elements by X-ray-fluorescence, (2) analyses of planktonic and benthic foraminifera, lithic grains and stable isotopic measurements (oxygen and carbon). We have focused on the long-term evolution of glacial stages (with special attention to terminations and Heinrich events). The results obtained confirm the close correlation between deep-sea sedimentation recorded on the Celtic margin and changes in the terrestrial environment of the adjacent continent. Heinrich layers have been identified in MIS 2, 3, 6 and 8. We note the occurrence of laminated facies within deglacial sequences deposited during Termination I and MIS 6. These facies are closely linked to disintegration phases of the British–Irish Ice Sheet (BIS). The laminations contain lower ice-rafted detritus (IRD) concentrations than the equivalent Heinrich layers and are linked to abrupt changes in sea-surface palaeotemperatures. We suggest that the laminations are formed by an annual cycle of meltwater and iceberg release from the disintegrating BIS generating cascading plumes of dense turbid meltwater coeval with IRD release.

Keywords: Celtic margin; glacial terminations; British–Irish Ice Sheet; laminated sediments

* Corresponding author.
E-mail addresses: mojtahid.meryem@caramail.com (M. Mojtahid), f.eynaud@epoc.u-bordeaux1.fr (F. Eynaud), s.zaragosi@epoc.u-bordeaux1.fr (S. Zaragosi), j.scourse@bangor.ac.uk (J. Scourse), jfb@ifremer.fr (J.-F. Bourillet), garlan@shom.fr (T. Garlan).
[1] Now at: Laboratory for the Study of Recent and Fossil bio-indicators, CNRS UPRES EA 2644, Angers University, 2 Boulevard Lavoisier, 49045 Angers Cedex, France.

0025-3227/$ - see front matter © 2005 Elsevier B.V. All rights reserved.
doi:10.1016/j.margeo.2005.07.007

1. Introduction

Not all the terminations which mark the abrupt transitions between the glacial and interglacial stages of the Quaternary (Broecker and van Donk, 1970) are accurately constrained. In the high latitudes of the North Atlantic Ocean, terminations are marked by abrupt changes of microfauna from polar to diversified subpolar assemblages (McIntyre et al., 1972) as a direct consequence of orbitally forced global warming. These transitions, which are also clearly expressed in temperate sediments of the North Atlantic Ocean, are coeval with marked palaeotemperature fluctuations and water mass reconfigurations (McIntyre et al., 1972; Ruddiman and McIntyre, 1976; Sarnthein and Tiedemann, 1990). These water mass changes are linked to global changes via the disruption of the Atlantic meridional overturning circulation (MOC) component of the thermohaline circulation (THC, e.g. Broecker et al., 1990).

The aim of this study was primarily to investigate the palaeoenvironmental history of terminations in the northern Bay of Biscay through the study of one of the longest cores ever retrieved in this area, core MD03-2692. This core covers the last three climatic cycles (with core base within Marine Isotopic Stage, MIS, 10) and provides, for the first time, an opportunity to document the last 360 ka in this area. One of the key attributes of sequences recovered from the Bay of Biscay is that they contain terrigenous material derived from the adjacent continent, enabling the identification of connections between the ocean, cryosphere (glacial collapse), continent and atmosphere. Previous studies in this part of the Bay of Biscay (Zaragosi et al., 2001; Locascio, 2003) have revealed the presence of a characteristic facies dominated by millimetric laminations and occurring recurrently across Terminations I and II. Such laminated facies were also present in core MD03-2692, to which we pay particular attention.

We have undertaken a multi-proxy investigation using physical, stratigraphical, geochemical, sedimentological, and micropaleontological tools, and have focused our work on identifying similarities and discrepancies between the different climatic cycles investigated. In particular we have analysed glacial stages containing evidence for abrupt events, including Heinrich events, and deglacial phases.

2. Present and past regional setting

Core MD03-2692 (46°50′ N, 9°31′ W) was retrieved from the Trevelyan escarpment (Fig. 1) in a water depth of 4064 m during the SEDICAR cruise onboard the oceanographic *RV Marion Dufresne II* of the Institut Polaire Paul-Emile Victor (IPEV). The scientific aims of this cruise (Bourillet and Turon, 2003) were to study sediment fluxes from estuaries towards the deep-sea during periglacial regimes (over the last few climatic cycles) including a detailed case study of "The Channel River/Manche system" (Bourillet et al., 2003; Gibbard and Lautridou, 2003; Lericolais et al., 2003). The Trevelyan escarpment, adjoining the Meriadzek terrace, is part of this fluvial system which extends from the southern North Sea to the Bay of Biscay. It comprises the continental shelf, the English Channel, a portion of the continental slope characterised by many erosive canyons, and a rise marked by the two recently discovered deep-sea turbidite systems, the Celtic and Armorican fans (Auffret et al., 1996; Droz et al., 1999; Zaragosi et al., 2000, 2001).

Core MD03-2692, 38.96 m in length, consists mainly of hemipelagic clays. Recent sedimentation is controlled by the local hydrography which is dominated by four water masses. The abyssal water mass is Lower Deep Water (LDW), a low salinity and low temperature water mass but with high silica content (van Weering et al., 1998; Frew et al., 2000; van Aken,

Fig. 1. (a) Physiography of the studied area. Bathymetric contour intervals are 50 m on the shelf (0–250 m), 500 m on the slope (500–4000 m) and 100 m on the deep-sea (4000–4900 m). The blue surface depicts the B.I.S. full glacial extension (after Stokes and Clark, 2001; Lambeck, 1995; Boulton et al., 1977); blue continuous arrows represent the Irish Sea Ice stream during the LGM (after Mc Cabe, 1998; Scourse et al., 2000 and Stokes and Clark, 2001). Red dotted line and red arrows represent Heinrich 1 ice limit and ice flows directions, respectively (after Bowen et al., 2002). The English Channel paleovalleys are also depicted for the oriental part (after Larsonneur et al., 1982) and the occidental part of the margin (after Bourillet et al., 2003) (Scilly glaciation after Scourse (1991)). (b) Location of the studied core and nearby cores with regards to the detailed geomorphology of the margin. (For interpretation of the references to colour in this figure legend, the reader is referred to the web version of this article.)

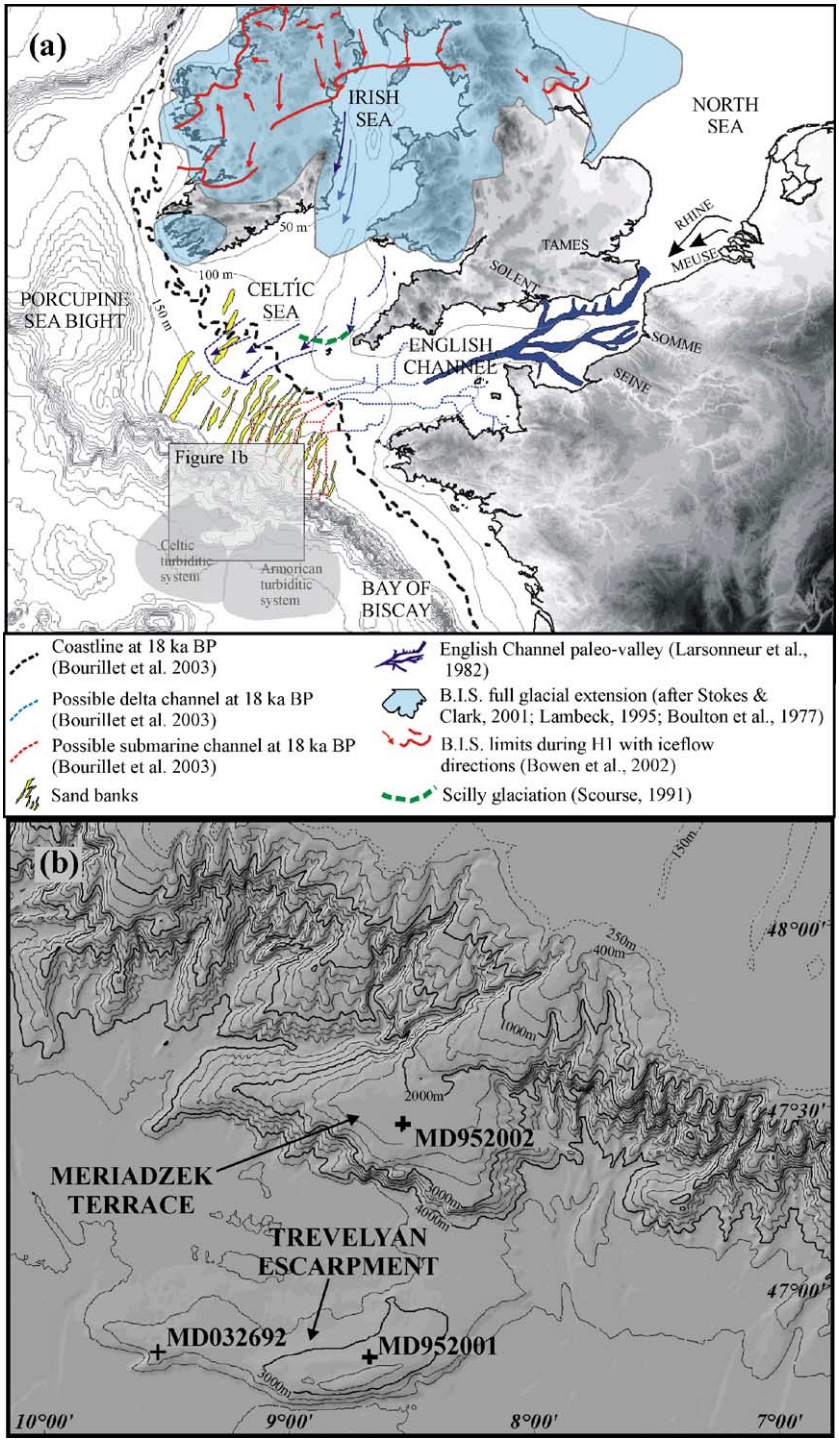
(a)
IRISH SEA
NORTH SEA
RHINE
MEUSE
TAMES
SOLENT
SOMME
SEINE
ENGLISH CHANNEL
CELTIC SEA
PORCUPINE SEA BIGHT
50 m
100 m
150 m
Figure 1b
Celtic turbiditic system
Armorican turbiditic system
BAY OF BISCAY
Coastline at 18 ka BP (Bourillet et al. 2003)
Possible delta channel at 18 ka BP (Bourillet et al. 2003)
Possible submarine channel at 18 ka BP (Bourillet et al. 2003)
Sand banks
English Channel paleo-valley (Larsonneur et al., 1982)
B.I.S. full glacial extension (after Stokes & Clark, 2001; Lambeck, 1995; Boulton et al., 1977)
B.I.S. limits during H1 with iceflow directions (Bowen et al., 2002)
Scilly glaciation (Scourse, 1991)
(b)
150m
250m
400m
1000m
2000m
3000m
4000m
MD952002
MERIADZEK TERRACE
TREVELYAN ESCARPMENT
MD032692
MD952001
48°00'
47°30'
47°00'
10°00'
9°00'
8°00'
7°00'

2000). This is overlain by Labrador Sea Water (LSW) and Mediterranean Outflow Water (MOW). At the surface, the influence of currents of the north-eastern branch of the Northern Atlantic Drift (NAD) leads to relatively high salinity and high temperature water. The hydrological dynamics influencing modern sedimentation in the area are critically reviewed in van Weering et al. (1998).

During the Quaternary, sedimentation in the area was directly influenced by terrigenous input from the adjacent European continent. Climatic conditions during the last few glacial stages were probably very similar to those of the Last Glacial Maximum (LGM, sensu EPILOG, Mix et al., 2001), the only glacial period for which the palaeogeography is well constrained in the area (Fig. 1a). During the LGM, the total ice volume accumulated on the continents reached more than double the current ice sheet volume (48.10^6 km^3 for the northern hemisphere according to Loutre and Berger (2003)), implying therefore a lowering of the sea-level of about 120 ± 10 m below the present day level (Fairbanks, 1989; Lambeck et al., 2002; Sidall et al., 2003). In the Bay of Biscay, the nearest ice sheet which developed during these glacial maxima was the British–Irish Ice Sheet, BIS (e.g. Mc Cabe and Clark, 1998; Scourse et al., 2000; Scourse and Furze, 2001; Richter et al., 2001; Bowen et al., 2002; Knight, 2004). Also, during cold stages of the last 500 000 yrs the Channel River flowed westwards from the southern North Sea along the centre of the English Channel. This palaeoriver was supplied via the connected drainage basins of modern rivers including the Seine, the Somme, the Solent and probably the Meuse, the Rhine and the Thames (Larsonneur et al., 1982; Gibbard, 1988; Lericolais, 1997). During sea-level low stands this river was in direct connection with some canyons on the slope (Le Suavé et al., 2000; Bourillet and Lericolais, 2003) at the edge of the continental shelf (200 m). These convergent canyons fed the two deep-sea fans (4500 m) constituted by the Celtic and Armorican turbiditic systems (Zaragosi et al., 2001; Bourillet et al., 2003).

During deglaciations, collapse of the BIS resulted in significant discharge of icebergs and meltwater. Both icebergs and meltwater were supplied via the Irish–Celtic seas and along the western Irish margin, and meltwater also via the Channel River. These fluxes were confluent along the Celtic margin (Fig. 1a), and thus supplied the deep-sea environments (Zaragosi et al., 2001). For the post-LGM deglaciation, the BIS collapse is well recorded through retreat phase push moraine formations on the west coast of Ireland and in the Irish Sea Basin (e.g. Mc Cabe and Clark, 1998; Bowen et al., 2002). Evidence for such iceberg and meltwater sources is also found in previously studied cores from the area, in which the terrigenous fraction is very largely dominated by quartz (e.g. Scourse et al., 1990, 2000). These minerals could result from the Palaeozoic formations (Devonian Old Red Sandstone, quartzite) which cover Ireland, parts of England (Cornwall, South Wales, coastal zones of Scotland) and even parts of the Celtic Sea (Richter et al., 2001; Zaragosi et al., 2001).

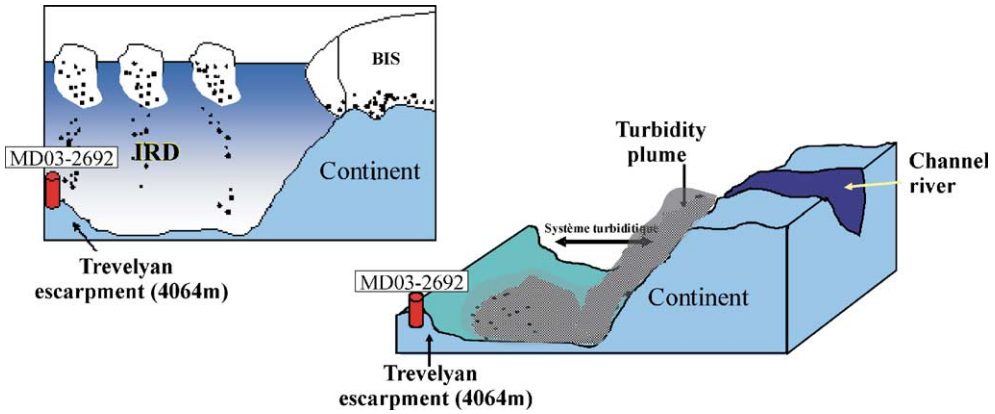

Fig. 2. Explanatory diagram of sources of the coarse detritical grains observed in the sediments of core MD03-2692.

The Trevelyan escarpment resulted from both the rifting Bay of Biscay segmentation and the Eocene compressive phase (Thinon et al., 2001) and is 500 m shallower than the surrounding deep-sea fans (Fig. 1b). This structure is physically disconnected from the continental slope and from the canyon network, and is therefore not subject to turbiditic sedimentation. However, coarse lithic deposits (>150 μm) are recurrently recorded in the core. These discrete events correspond to "Heinrich" and/or "Heinrich like events" (Heinrich, 1988; Bond et al., 1992; van Kreveld et al., 1996) distributed throughout the 360 ka covered by the core. Previous studies in the area (Zaragosi et al., 2001) have already demonstrated that coarse lithic grains are primarily supplied by ice-rafting (including icebergs directly liberated from the BIS) and not by turbidity currents: this interpretation is conceptualised in Fig. 2.

3. Materials and methods

3.1. Physical and geochemical measurements

3.1.1. Physical properties

Magnetic susceptibility, gamma density and reflectance were measured onboard (Bourillet and Turon, 2003). Thin slabs were sampled at the Department of Geology and Oceanography at the University of Bordeaux 1 (UMR 5805 EPOC) and analysed by X-ray using the SCOPIX image-processing tool (Migeon et al., 1999).

3.1.2. Major elements and stable isotopic measurements

Within the framework of the PALEOSTUDIES EU-project (Contract No.: HPRI-CT-2001- 0124), the measurement of major elements has been undertaken by CORTEX X-ray-fluorescence (XRF) analysis at 2 cm resolution. Among the 14 major elements measured using this method, only those which can be clearly related to climatic variability (i.e. Ca, Sr, Fe and Ti) are discussed here.

Preliminary graphical comparison of the reflectance record obtained onboard with the SPECMAP curve (Martinson et al., 1987) indicates that the studied sections extend from Marine Isotopic Stage (MIS) 10 to MIS 1. Since this correlation remains approximate, we measured $\delta^{18}O$ on three different species of benthic foraminifera (*Uvigerina peregrina*, *Pullenia bulloides* and *Planulina wuellerstorfi*) at a resolution of 10 cm to validate and detail the preliminary stratigraphic framework.

Some of the analyses (200 measurements) were carried out at the Department of Geology and Oceanography at the University of Bordeaux 1 (UMR 5805 EPOC) using an *Optima Micromass* mass spectrometer. To complete the record, 100 samples were also analysed at the School of Ocean Sciences, University of Wales, Bangor, using a *PDZ Europa Geo 20/20* Isotope Ratio Mass Spectrometer with an automated carbonate system (CAPS).

The $^{18}O/^{16}O$ ratio is integrated in the calcite of the foraminifera tests with isotope fractionation dependent on the ambient water temperature and the settlement depth of the test. Thus, depending on the species considered, this ratio varies. Accordingly, Duplessy et al. (1983) developed a $\delta^{18}O$ correction factor for different species. For *U. peregrina* and *P. bulloides* we have used a correction of 0‰ as these species calcify in equilibrium with seawater. For *P. wuellerstorfi*, the correction applied is +0.64‰.

3.2. Characterization of the coarse detrital fraction >150 μm

The core was subsampled every ten centimetres. Each subsample of 8 cm^3 was weighed, dried overnight and then weighed to obtain dry weight (gram dry sed.). The subsamples were then washed through a 150 μm sieve. The residual fraction was dried and weighed. This fraction comprises primarily biogenic benthic and planktonic foraminifera and coarse terrigenous detrital grains (potentially ice-rafted detritus, IRD).

3.2.1. Biogenic characterization

Known aliquots of the dried residues were counted for their planktonic and benthic foraminiferal content to obtain absolute abundances for these two groups per gram of dry sediment. Counting of planktonic foraminifera focused on the species *Neogloboquadrina pachyderma* sinistral to obtain relative abundances (percentages) of this species of the total planktonic fauna. *N. pachyderma* s. is a morphotype which today dominates the polar environments of the

North Atlantic Ocean (Bauch et al., 2002) and is adapted to cold sea-surface temperatures. High percentages of this species in the sediments of the Bay of Biscay are associated with the incursion of polar water masses (Auffret et al., 1996).

3.2.2. Terrigenous characterization

The coarse detrital grains were characterized and counted from all samples. These grains include all the lithic grains greater than 150 μm and include Ice-rafted Detritus (IRD) which indicate iceberg melt fluxes (i.e. Heinrich events, Manighetti and McCave, 1995).

We have defined five classes for counting in order to facilitate source identification: quartz (the dominating element), rock debris, volcanic grains, carbonates and others (including feldspars and micas). Results are presented as percentages and concentrations (number of grains/gram dry sediment).

3.3. Stratigraphy

The $\delta^{18}O$ composite curve obtained on the basis of stable isotope measurements was correlated (Fig. 3), primarily peak to peak, using the "AnalySeries" software (Paillard et al., 1993) with the SPECMAP curve (Martinson et al., 1987). This stack was selected given that the study covers the last 360 ka. Data were downloaded from NCDC (ftp://ftp.ncdc.noaa.gov/pub/data/paleo/paleocean/specmap/). The age scale obtained using this method was tested against the age scale obtained (using the same software) with the correlation of the calcium curve (obtained by XRF) with the SPECMAP curve. The result of this comparison (Fig. 4, Table 1) highlights the stratigraphical significance of the long-term variation in Ca in this area. A lag of age control points exists, however, for the last 70 ka, a period marked by high-frequency climatic variations beyond the resolution of the SPECMAP data. This was solved using the *N. pachyderma* s. percentage curve obtained on the adjacent MD95-2002 core (Zaragosi et al., 2001; Auffret et al., 2002) which shows clear similarity with the percentage curve of the same species in our core. Since the age scale of MD95-2002 is well constrained over the last 70 ka (11 ^{14}C dates between 0 and 30 ka, Grousset et al., 2000; Zaragosi et al., 2001; Auffret et al., 2002), we applied a peak to peak correlation

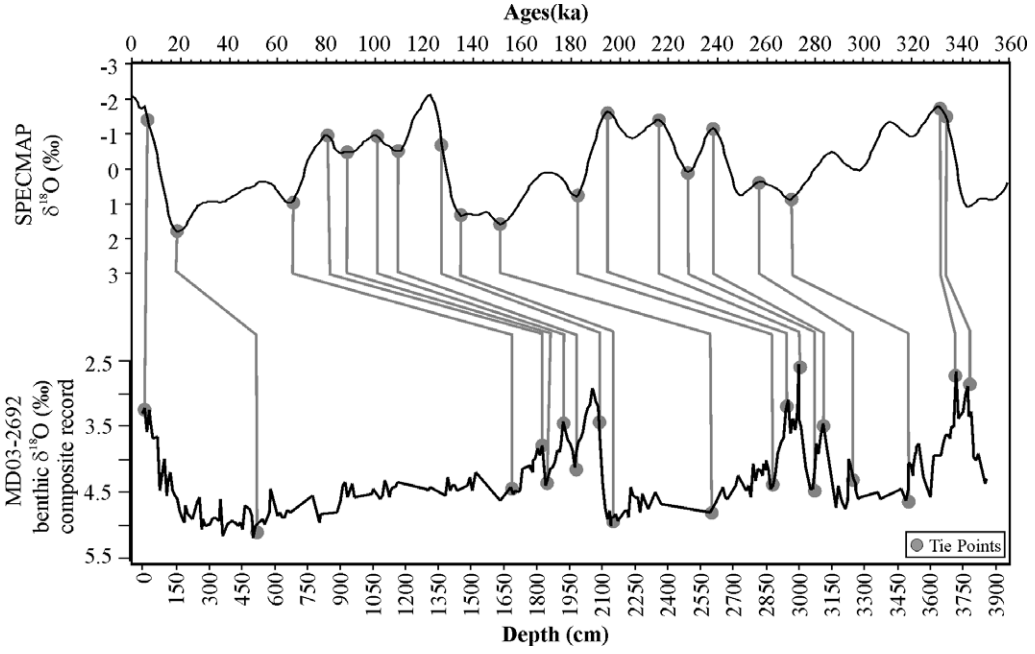

Fig. 3. Stratigraphic correlation in between the MD03-2692 $\delta^{18}O$ benthic record and the SPECMAP stack (ftp://ftp.ncdc.noaa.gov/pub/data/paleo/paleocean/specmap/). Tie-points have been positioned using the software "analyseries", Paillard et al. (1993).

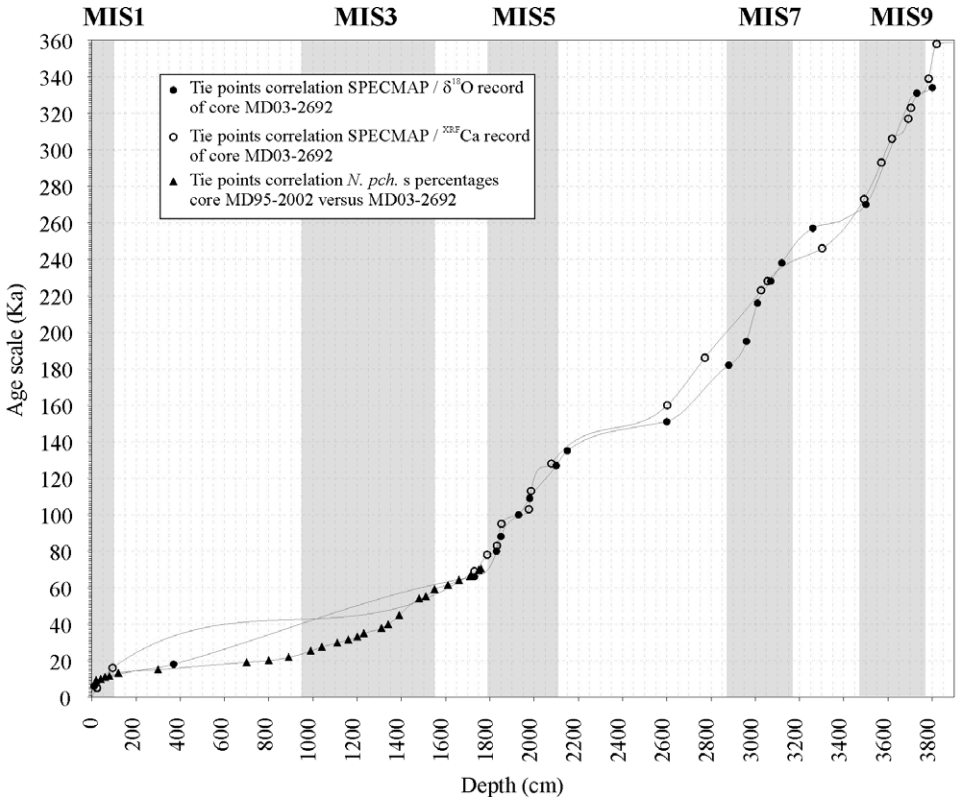

Fig. 4. MD03-2692 age model for the last 360 ka. The age model is based on the correlation with SPECMAP (δ^{18}O benthic record) in between 360 and 70 ka and on the correlation of the *N. pachyderma* s. percentages with the well-dated proximal core MD95- 2002 (Zaragosi et al., 2001; Auffret et al., 2002) for the younger part (curve with black tie-points).

with the "AnalySeries" software to obtain a precise age model for this period (Fig. 4).

3.4. Micromorphological and sedimentological observations

Thin section sediment slides provide data on the microstructure of the sediment by optical microscopy reflection techniques (Bénard, 1996). Sediment slides were selected according to the relevance of the core section for our study. Preliminary evaluations were based on X-ray images which enabled location of the laminae and Heinrich events. The X-ray observation of Heinrich layers was complemented by the location of magnetic susceptibility peaks (Fig. 5), which in the Bay of Biscay generally correspond to Heinrich events (Grousset et al., 2000).

We produced seven sediment slides, with numbers 1, 4, 5 and 6 in the laminated facies and numbers 2, 3 and 7 positioned at the level of two large magnetic susceptibility peaks. The measurement of particle size was carried out by diffractometry using a Malvern instrument. This instrument refracts light according to an angle which is a function of particle size. Because it overestimates the size of clays, the practical detection limit of the silt–clay boundary is at 10 μm instead of 4 μm, which is the theoretical limit (Weber et al., 1991). Grain-size measurements were undertaken on plates 4, 5 and 6 (Fig. 5).

4. Results

4.1. XRF results (Fig. 6)

Fig. 6 highlights the obvious similarity between, on the one hand, the variability of Ca and Sr, and, on

Table 1
List of the tie-points used to construct the MD03-2692 age scale

Tie-points	
Depth (cm)	Time (kyr BP)
Ca_MD03_92 versus $\delta^{18}O$_SPECMAP	
24	5
94	16
1730	69
1788	78
1832	83
1852	95
1976	103
1986	113
2078	128
2602	160
2772	186
3026	223
3056	228
3302	246
3492	273
3570	293
3618	306
3692	317
3704	323
3784	339
3820	358
$\delta^{18}O$_MD03_92 versus $\delta^{18}O$_SPECMAP	
10	6
370	18
1730	66
1830	80
1850	88
1930	100
1980	109
2100	127
2150	135
2600	151
2880	182
2960	195
3010	216
3070	228
3120	238
3260	257
3500	270
3730	331
3800	334

Tie-points		
Depth (cm)	Time (^{14}C-kyr BP)	Time (CAL-kyr BP)[a]
%N. pachyderma s. MD03_92 versus MD95_02		
10	6.56	7.42
20	9.25	10.35
40	9.76	11.02
60	10.93	12.73
80	11.50	13.43
120	13.19	15.48
300	15.04	17.71
700	19.03	22.45
800	20.01	23.59
890	21.76	25.63
990	25.32	
1040	27.44	
1110	29.70	
1160	31.39	
1200	33.07	
1230	34.91	
1310	37.73	
1340	39.85	
1390	44.79	
1480	53.86	
1510	55.14	
1550	59.00	
1610	61.44	
1660	64.08	
1710	66.15	
1750	69.62	
1760	70.31	

[a] Bard polynomial conversion from Bard (1998).

the other, between Fe and Ti, and also the anticorrelation between these two groups. Indeed, though Ca and Sr are positively correlated (Fig. 6) they are characterised by different absolute values. Ca attains about 6000 cps (counts/second) during the warm isotopic stages and about 1500 cps during the cold ones, and Sr 120 cps during the interglacials and 40 cps during the glacials.

In this sequence, Ca is primarily sourced mainly from biogenic $CaCO_3$ as suggested by the covariation of this parameter with the foraminiferal absolute abundances. This is also supported by the Sr data. It is well established that Sr (alkaline earth element) is fixed by calcifying organisms at the same time and in the same way as Ca. Sr is routinely used in marine environments as a marker of a strictly biogenic origin because it is fixed only by living organisms (Martin et al., 2004). Conversely, Ca can be supplied from terrigenous sources (including in feldspars, detrital carbonates and clays).

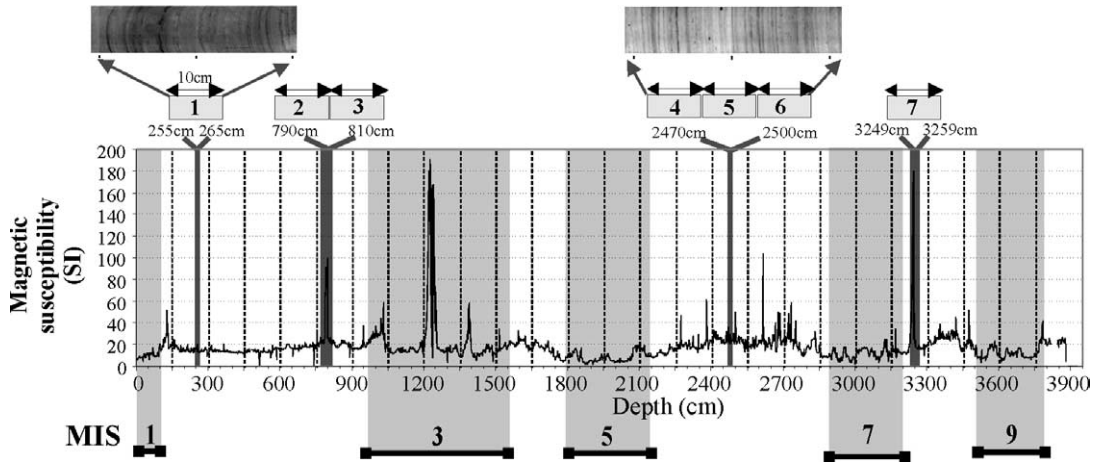

Fig. 5. Magnetic Susceptibility (MS) record (onboard data, SI) of core MD03-2692. Grayed zones mark the interglacial marine isotopic stages. Sediment slides taken for microstructure analysis are also located on this figure (slide number 1 to 7) with some X-ray imagery selected sections. N.B.: An anomaly occurs during the onboard data acquisition for the section of the core in between 580 and 680 cm. We corrected it, adding the core background value of 15 SI.

Our record shows the anticorrelation of Fe and Ti with Ca and Sr. During interglacial stages, the Fe values vary around 1000 cps and Ti about 30 cps. Conversely, during glacial stages, these values increase to about 6000 cps for Fe and 200 cps for Ti. The difference of ranges between these two elements arises from the fact that Ti is less abundant than Fe. During glacial stages the increase in Fe in parallel to Ti can be explained by the fact that these elements are common constituents of rocks such as gneisses or schist and therefore primarily indicate a terrigenous continental source. In addition, during glacial stages, thermal gradients are higher, generating an intensification in the atmospheric circulation (Joussaume, 2000) and thus more significant transport of dust generally rich in iron.

4.2. Characterization of the sedimentary fraction >150 μm

4.2.1. Biogenic fraction (planktonic foraminifera) (Fig. 7)

Throughout the entire record the mean number of planktonic foraminifera exceeds 1500 individuals per gram of dry sediment. During interglacial stages, planktonic foraminiferal abundances increase significantly (up to 4500 individuals per gram of dry sediment). The proportion of benthic to planktonic foraminifera is very small. Their absence in some samples suggests adverse conditions for their survival in this area.

The relative abundance of the polar species *N. pachyderma* s. permits the discrimination of specific events in the record: (1) Interglacial stages (MIS 1, 5, 7 and 9) are characterized by very small percentages or even absence of this polar taxon, evidencing subpolar to temperate (or even warmer) assemblages during these intervals. This micropalaeontological signature of high sea-surface temperatures is supported by light values of benthic $\delta^{18}O$ (3‰) related to low ice volume. Conversely, glacial stages are characterized by higher percentages of this taxon and heavy values of $\delta^{18}O$ (around 4.5‰). (2) Higher frequency climatic oscillations are clear within the glacial stages with cold events (where *N. pachyderma* s. percentages generally exceed 80%) and cool events (where *N. pachyderma* s. percentages rarely exceed 20%, Fig. 7). Benthic $\delta^{18}O$ values do not present marked variations (from 4‰ to 5‰) during these events compared to the difference between glacial and interglacial values, suggesting a minor impact on global sea-level. (3) The two distinctive sequences of laminated sediments are also clearly depicted in the *N. pachyderma* s. percentages as they constitute parts of the record where percentages exceed 95%. The first sequence is situated between 150 and 300 cm and is dated approximately between 15 and 17 ka BP, and the second is between 2400 and 2800 cm and is dated approximately between 145 and 153 ka BP.

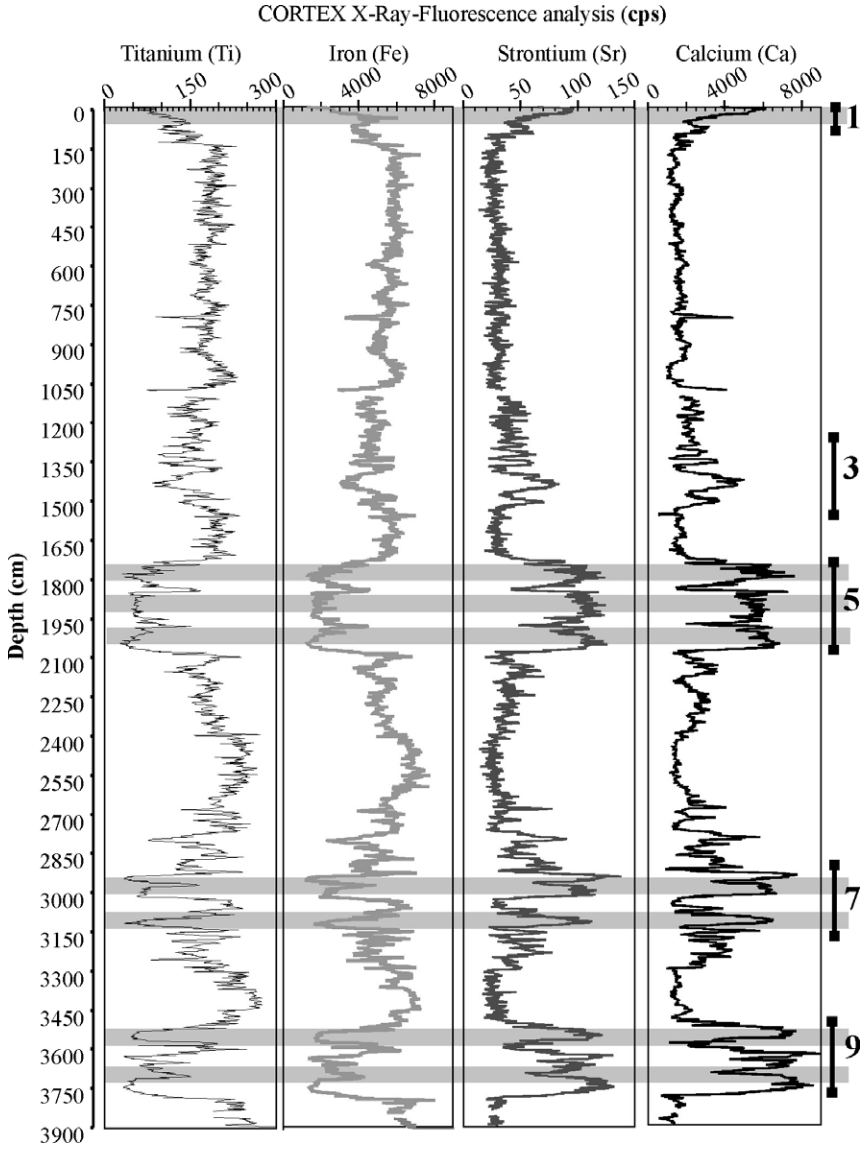

Fig. 6. Ca, Sr, Fe and Ti records obtained by XRF (grayed zones mark the interglacial climatic optima).

4.2.2. Terrigenous fraction (Fig. 8)

The coarse sediments (>150 μm) are characterized by a high diversity and variability of detrital grains (Fig. 8). This figure also shows the number of laminae per centimetre and the magnetic susceptibility (MS) measured onboard. Three categories of coarse grains are abundantly represented. Quartz dominates the record (with 69.2% on average), followed by rock fragments and other lithics. The remaining categories, including volcanic grains and detrital carbonates, are present only in very small proportions. We note that the magnetic susceptibility peaks correspond generally to coarse detrital grain concentration peaks (for example 2409 grains/g dry sed. at 1230 cm core depth).

The variability in these concentrations enable us to identify, in the same way as it has been done with *N. pachyderma* s. percentages, isotopic stages and isolated specific events: (1) During the interglacial stages, we observe a marked reduction or even an absence of coarse detrital grains accompanied by a

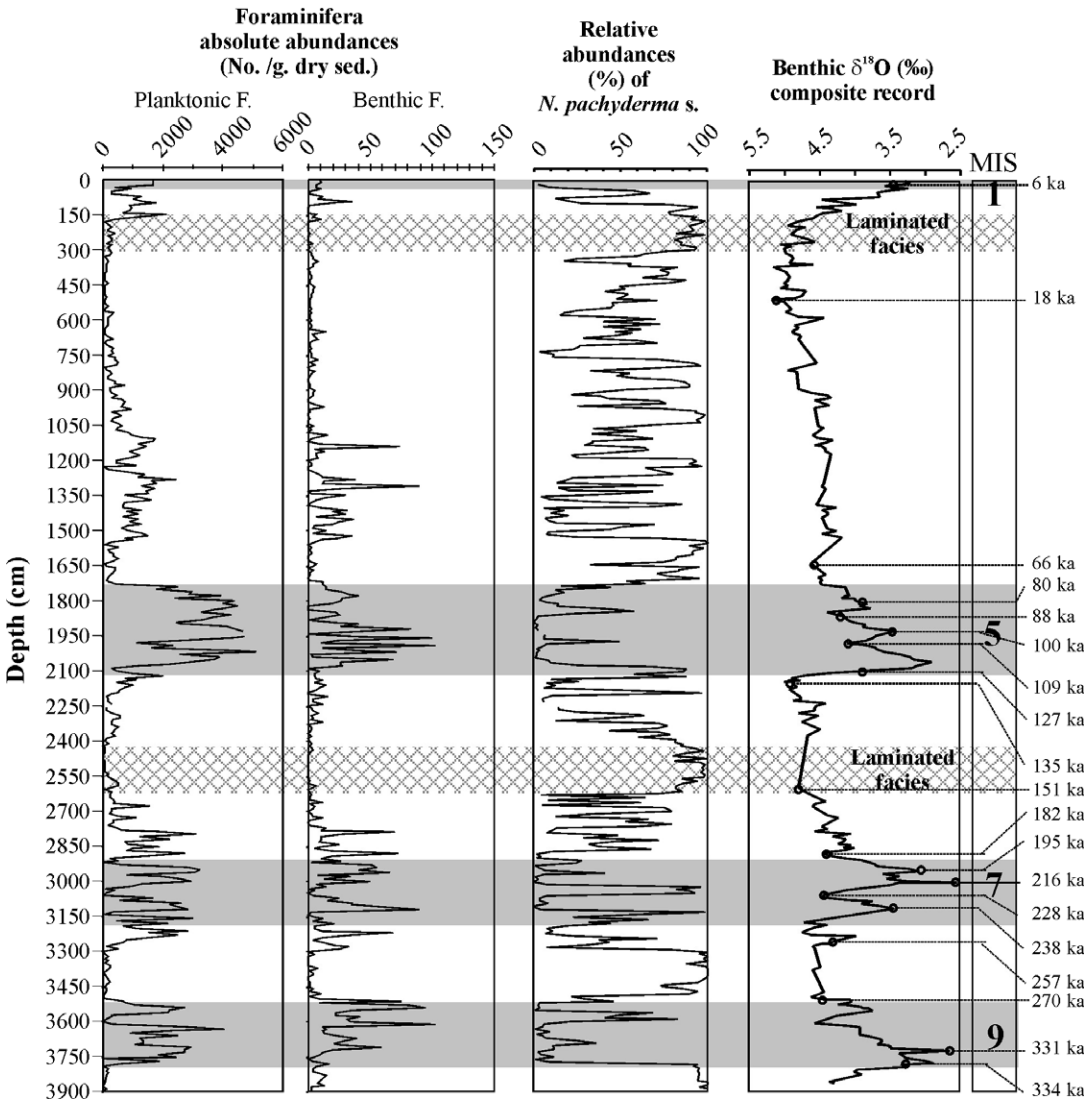

Fig. 7. Results of the foraminifera microfauna characterization. Planktonic and benthic foraminifera have been counted separately. Counts of the species *Neogloboquadrina pachyderma* s. allow us to obtain relative abundances of this proxies versus the planktonic foraminifera total assemblage. Ages indicated on the right part of the graph are those used as tie-points for the construction of the age model (correlation with SPECMAP δ^{18}O benthic record).

reduction in the magnetic susceptibility values which are themselves a function of the detrital fraction (Thouveny et al., 2000). (2) Conversely, during the glacial stages, the concentrations of the grains increase in parallel with the magnetic susceptibility. In this part of the Bay of Biscay, these coeval peaks have been demonstrated to represent Heinrich events, massive iceberg discharges from the Laurentide Ice Sheet (Grousset et al., 2000; Auffret et al., 2002). During MIS 2 and 6, the presence of laminated sediments is characterized by the predominance of the polar taxon *N. pachyderma* s. (see Section 4.2.1), by an increase in the concentration of quartz grains (with more than 80%; Fig. 8), and both sequences are preceded by very low concentrations of coarse detrital grains at the two levels (between 300 and 750 cm for the MIS 2 laminae event and between 2850 and 3100 cm for the MIS 6 event).

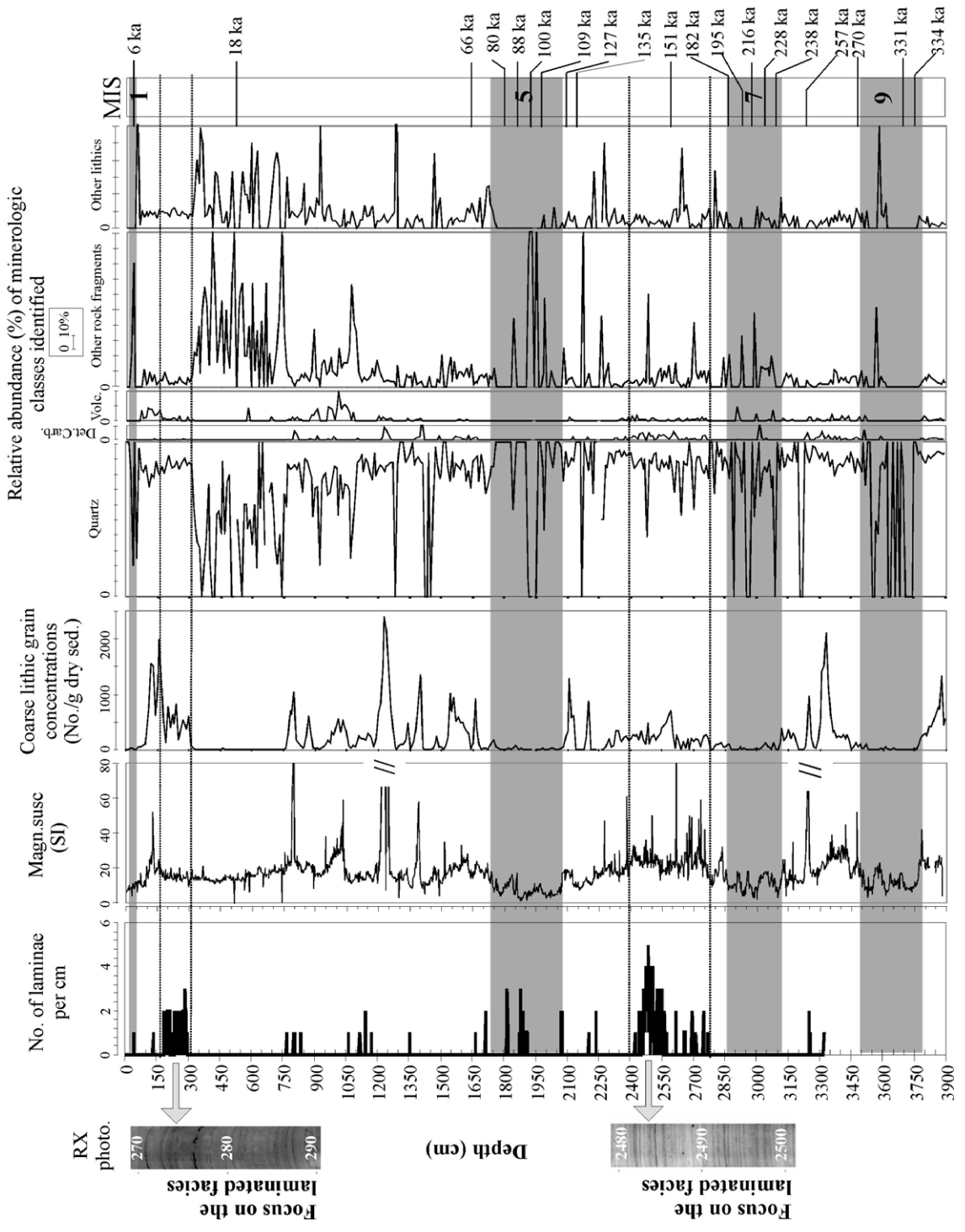
MIS
6 ka
18 ka
66 ka
80 ka
88 ka
100 ka
109 ka
127 ka
135 ka
151 ka
182 ka
195 ka
216 ka
228 ka
238 ka
257 ka
270 ka
331 ka
334 ka
Relative abundance (%) of minerologic classes identified
0 10%
Other lithics
Other rock fragments
Volc.
Det.Carb.
Quartz
Coarse lithic grain concentrations (No./g dry sed.)
Magn.susc (SI)
No. of laminae per cm
RX photo.
Focus on the laminated facies
Depth (cm)

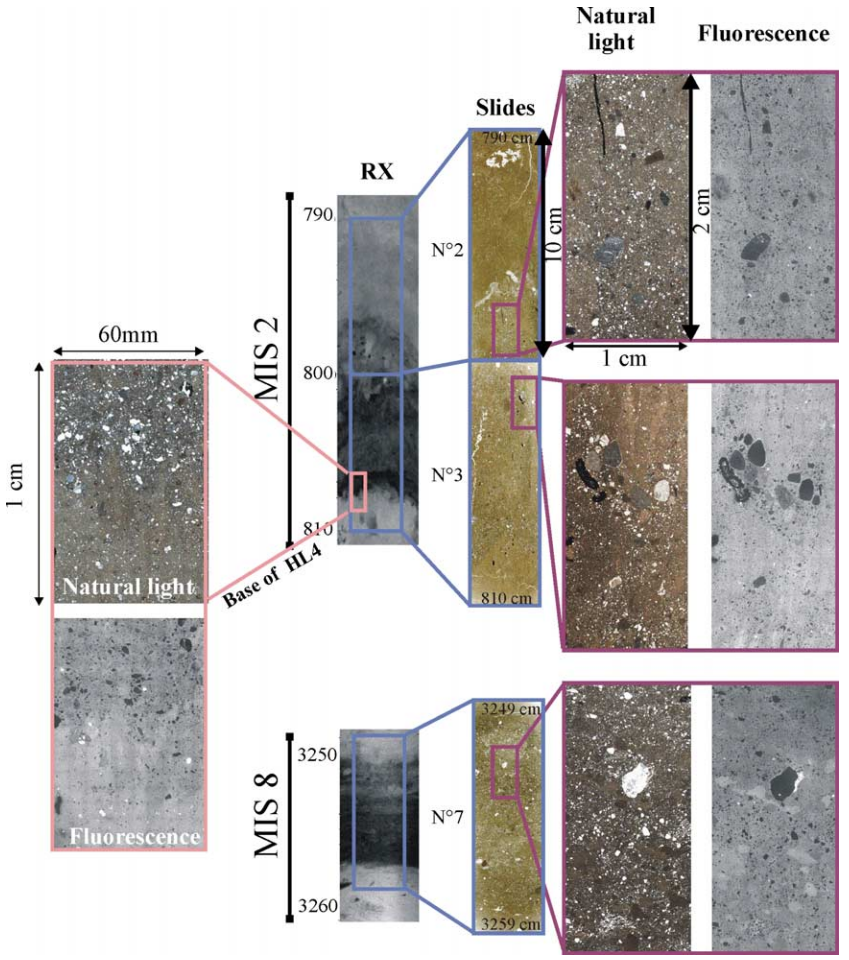

Fig. 9. Microphotography of the indurations of sediments corresponding to typical "Heinrich" events sensu Heinrich (1988) and Bond et al. (1992): HL4 example and microphotography of an "Heinrich like" event of MIS8.

4.3. Results of the sediment slide observations

4.3.1. Heinrich events (Fig. 9)

"Heinrich events" are abrupt episodes characterised by layers of coarse detrital IRD in sediments of the North Atlantic Ocean. These events result from the massive calving of icebergs in relation to the sudden and periodic collapse of the peri-arctic ice sheets during the glacial period (Heinrich, 1988; Bond et al., 1992). For the last 70 ka, 6 Heinrich events (HL1 to HL6) have been identified. Maximum concentrations of coarse lithic grains have been recognised within the "Ruddiman belt" (40–55°N, Ruddiman, 1977). These events are found in sedimentary sequences of the Bay of Biscay (Grousset et al., 2000; Zaragosi et al., 2001) and are well recorded in core MD03-2692. These layers are also characterized by a net increase in the abundances of the polar planktonic foraminifer *N. pachyderma* s., and a lightening in the surface water oxygen isotopic ratio due to the input of freshwater.

Fig. 8. Number of laminae per centimetre (counts based on the X-ray imagery analysis) plotted versus MS onboard data and the records of the coarse (>150 μm) lithic fraction (grains concentrations—No./gram dry sed., relative abundances of the mineralogic classes with a focus on Quartz, detritical carbonates, volcanic glasses and ash, other rocks and lithics). Zooms on laminated section of MIS2 and MIS 6 are depicted on the left part of the figure. Ages indicated on the right part of the graph are those used as tie-points for the construction of the age model (correlation with SPECMAP $\delta^{18}O$ benthic record).

The six most recent events have been studied in detail, but older "Heinrich like events" can be identified at least back to 260 000 yrs before present–yr BP– (Grousset et al., 1993; McManus et al., 1994; Verbitsky and Saltzman, 1995; van Kreveld et al., 1996; Chapman and Shackleton, 1998; Eynaud et al., 2000; Thouveny et al., 2000; Moreno et al., 2002).

These events are observed in X-ray images by their extremely dark and bioturbated facies. On sediment slides (Fig. 9), they are characterized primarily by a great diversity of coarse detrital grains consisting of angular silts, sands and gravels. Such grains could not have been supplied by turbidity or gravity flows on the Trevelyan escarpment and can therefore be identified as IRD. The base of these events is distinct, marking an abrupt change from a primarily argillaceous sedimentation to a layer characterised by high quantities of coarse detrital grains.

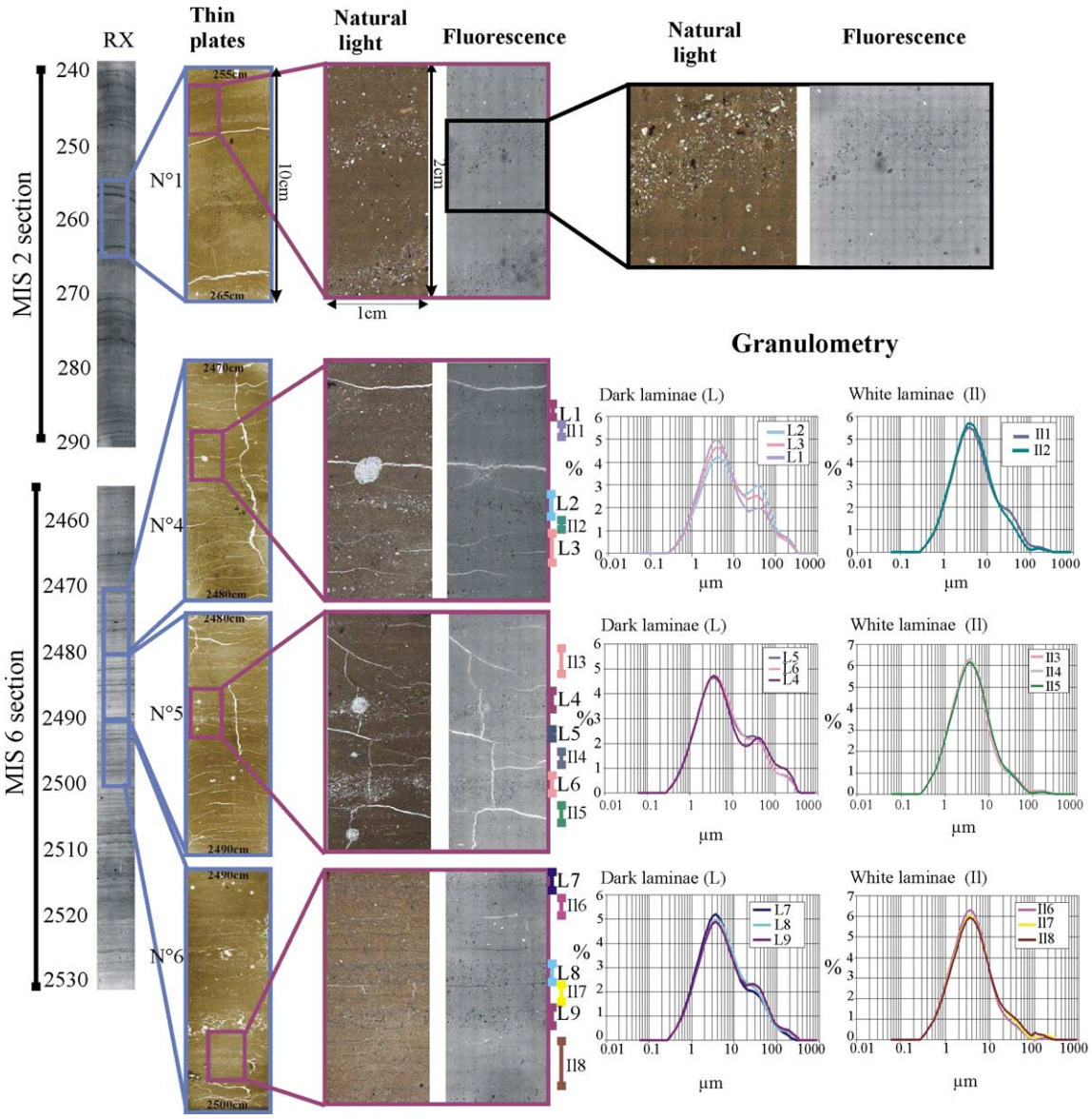

Fig. 10. Microphotography of the indurations of laminated sediments compared to the grain-size measurements undertaken on the laminae.

4.3.2. The laminae (Fig. 10)

Fig. 10 shows the presence of millimetric to centimetric sized laminations, evidenced by light and dark couplets on X-ray imagery. Microscopic analysis of the structure reveals obvious grain-size differences in between light and dark laminae; this interpretation is supported by grain-size measurements. The granulometry of the light laminae is bimodal, with a main mode at 4 μm and a secondary very small one at 150–180 μm, confirming that these are primarily composed of clays. The granularity of the dark laminae is trimodal with a significant mode at 4 μm, a secondary mode at 40 μm and a third mode at 200 μm, which suggests that these are composed of the same material as the light laminae but with the addition of coarse detrital silt and sand grains. The coarser grains do not present any apparent graded bedding.

5. Discussion

Fig. 11 compiles the most significant proxy records from core MD03-2692 for the last 360 000 yrs plotted against insolation data for 65°N (Berger and Loutre, 1991) as this parameter is now recognised to represent

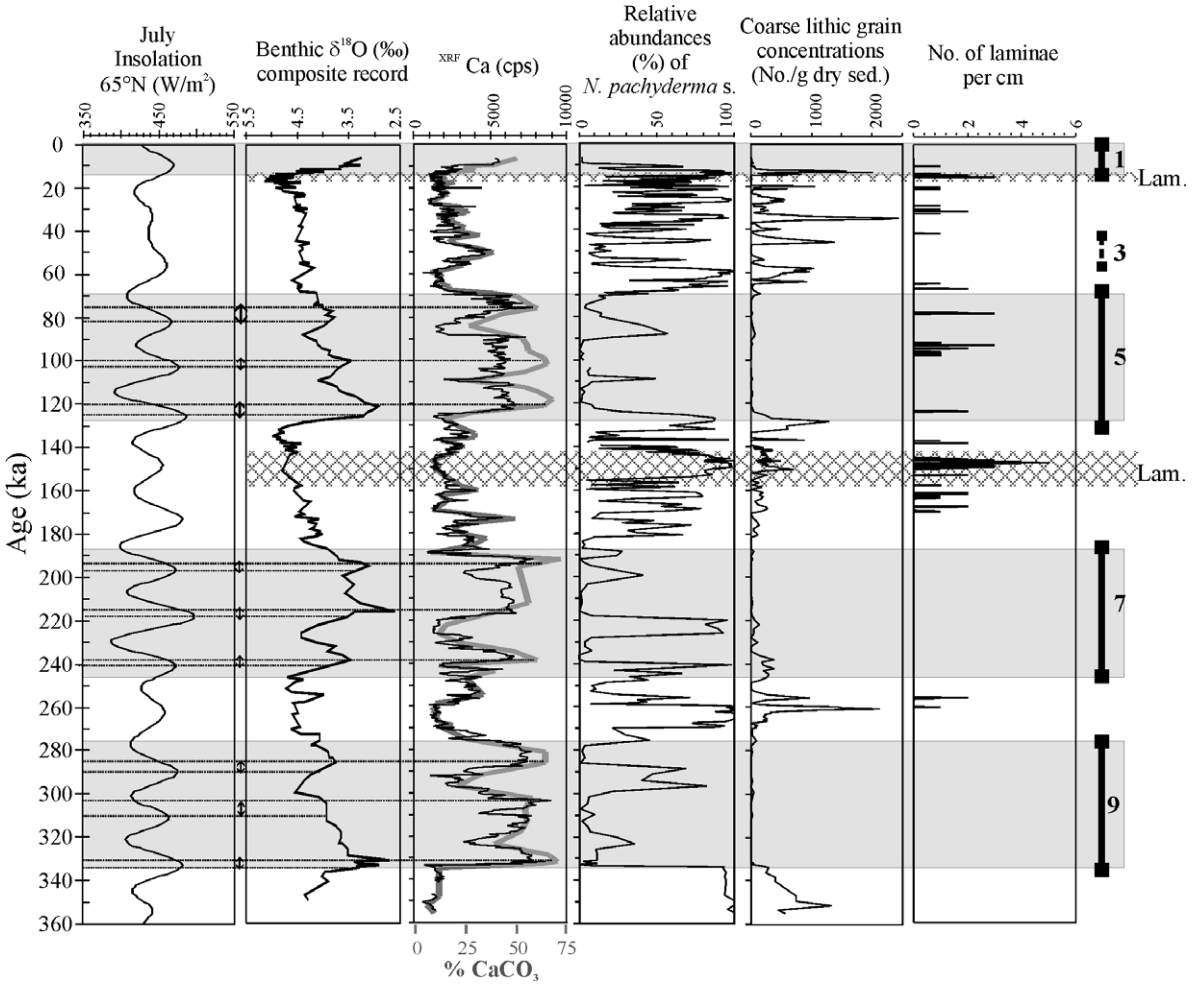

Fig. 11. Compilation of paleohydrological results obtained on core MD03-2692 (benthic $\delta^{18}O$; ^{XRF}Ca, *N. pachyderma* s. percentages, concentrations of coarse detritic grains and the number of laminae per centimetre) versus the July Insolation curve at 65°N (Berger and Loutre, 1991). Dotted lines on the left part of the figure show shifts between Insolation, $\delta^{18}O$ and ^{XRF}Ca.

the solar forcing of changing global climate (e.g. Imbrie et al., 1993). Interglacial stages (MIS 1, 3, 5, 7 and 9) are marked by a general climatic warming which follows an increase in the insolation at 65°N. For these stages, lightening of the benthic $\delta^{18}O$ values (Fig. 11) is associated with melting of the ice sheets and sea-level rise [a strong contribution of freshwater]. The increase of Ca in the sediments also supports high sea-surface temperatures, as this is primarily due to higher biogenic carbonate fluxes. During glacial stages (MIS 2, 4, 6, 8 and 10), values of $\delta^{18}O$ are heavier. The reduction in Ca and $CaCO_3$ content mark dilution (high abundance of detrital material) and/or a reduction in the carbonate productivity signal. The foraminiferal species that dominates these stages is the polar taxon *N. pachyderma* s., clearly marking cold surface water incursions. For these stages, the increase in Fe covaries with Ti (Fig. 5).

In examining the detailed phasing between these various parameters (insolation, $\delta^{18}O$ and Ca) we note, however, that they are not completely synchronous (Fig. 11). There is a distinct lag following each insolation peak before there is a response in foraminiferal benthic $\delta^{18}O$. This delay is in our record as large as 4 to 5 ka (start of MIS5). However the insolation peak corresponds to the "midpoint" of the $\delta^{18}O$ slope, which implies that when insolation is at a maximum, ice melting is accelerated.

It is worth noting the obvious difference in coarse lithic grain concentrations between the studied glacial stages. This suggests non-analogue situations between different glacial stages regarding the sources of these lithic fragments.

5.1. MIS 2

Our results (Fig. 12) conform to previous observations made on sequences from the same area of the Bay of Biscay (Grousset et al., 2000; Zaragosi et al., 2001; Auffret et al., 2002).

5.1.1. "*Heinrich events*"

These levels are distinguished by (Fig. 12) a high concentration of coarse detrital IRD grains, a large increase in percentages of the polar taxon *N. pachyderma* s. and peaks in magnetic susceptibility. Other indicators noted by other workers, notably a reduction in benthic $\delta^{18}O$ and $\delta^{13}C$ (Vidal et al., 1997; Bard, 2002), have not been recorded because of the paucity of benthic foraminifera in the HLs record.

5.1.2. The Last Glacial Maximum (LGM)

Recent studies of the LGM in the Bay of Biscay (Zaragosi et al., 2001) have revealed the presence of several "warm" events during this period long considered stable and cold. These events have been detected using dinocyst assemblages as a proxy for the Northern Atlantic Current. This Current, the northern branch of the Gulf Stream, transports warm water from the tropics northwards, and produces mild and moderate climatic conditions at the latitude of the Bay of Biscay. Within the framework of our study, these warm events are also recorded in the core through the collapse in *N. pachyderma* s. percentages (Fig. 13). During these events the percentages of the *N. pachyderma* s. do not exceed 20%, values comparable to those at the present day that characterise North Atlantic temperate sediments. Synchronously, benthic $\delta^{18}O$ values are slightly lighter. Based on the earlier dinocyst evidence these events have been interpreted as periods during which the intrusion of the Northern Atlantic Current was intensified, with increased heating causing a partial melting of the proximal BIS (Zaragosi et al., 2001).

5.1.3. The presence of laminated facies at the start of the last deglaciation

Laminated sediments that mark the beginning of HL1 are well recorded in core MD03-2692. Laminae in the same stratigraphic position have already been observed from adjacent cores: MD95-2001 and MD95-2002 (see Fig. 1 for locations). Such laminated facies have been interpreted as related to seasonal melting events of the BIS caused by a climatic warming at the end of the LGM (Fig. 13) linked to the insolation maxima at the onset of the last deglaciation (Fig. 12) (Zaragosi et al., 2001). Similar rapidly deposited laminated sediments dated between 18 and 21 cal. ka BP have also recently been reported from the Northern North Sea and the Southern Norwegian Sea (Lekens et al., 2005). These have been attributed to suspension plume deposits associated with the disintegration of the Norwegian Channel Ice Stream during HL1.

These events are probably associated with the Heinrich "precursors" which have been identified

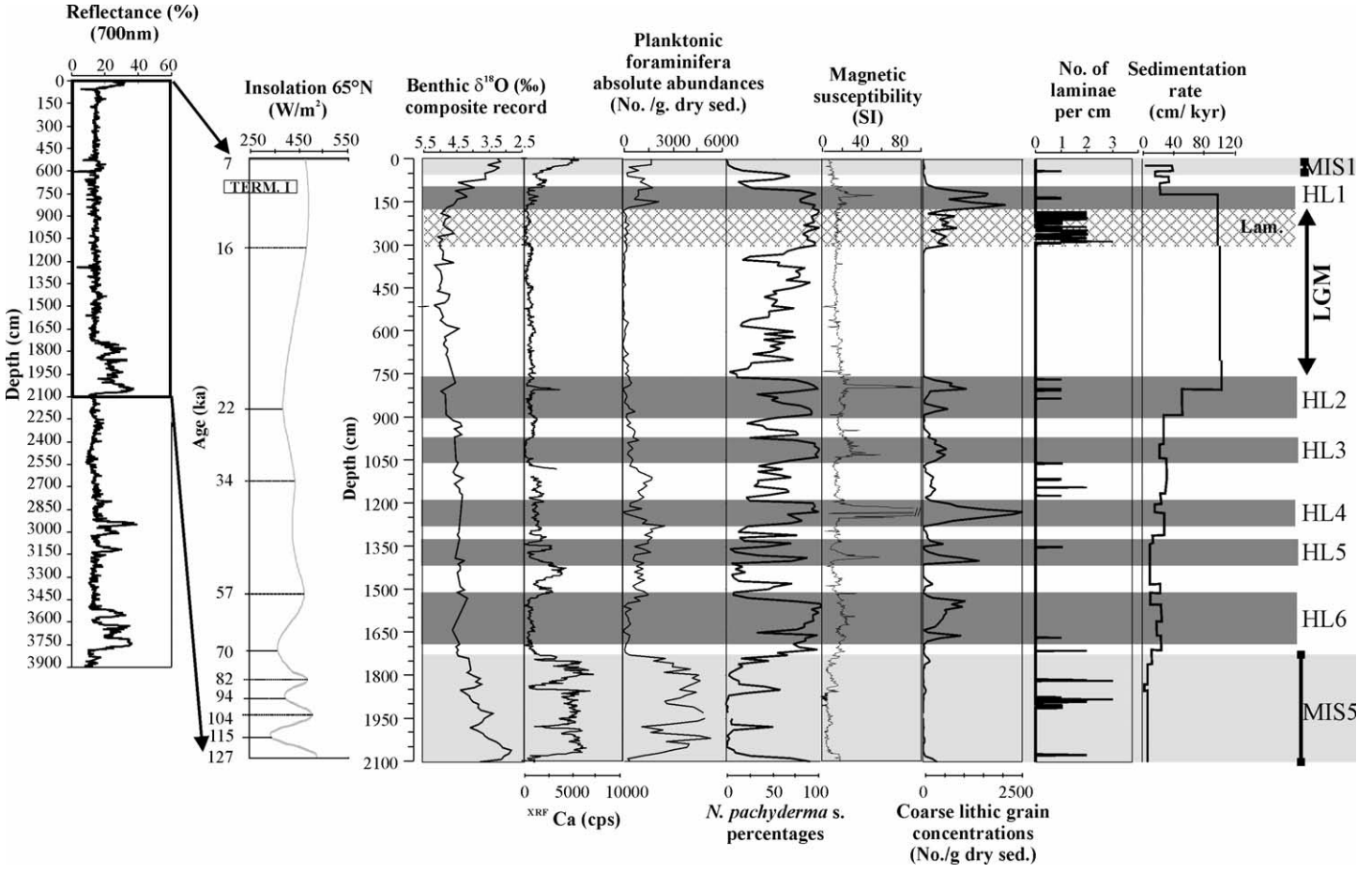

Fig. 12. Synthetic figure summarizing results obtained on the last climatic cycle. Data are plotted along depth in the core to avoid graphic distortion. Some age pointers are localized on the 65°N July insolation curve for each inflexion point of this parameter. Termination I onset was positioned according to Sarnthein and Tiedemann (1990). Dark gray bars mark "Heinrich" events, from HL1 to HL6.

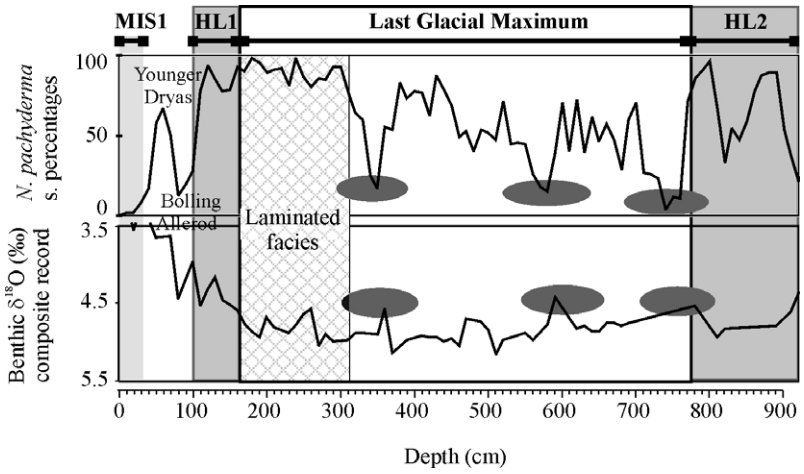

Fig. 13. Details of the 3 "warm" events during the LGM (sensu Mix et al., 2001) as recorded by *N. pachyderma* s. percentages and benthic $\delta^{18}O$. Worth noting is that, according to the *N. pachyderma* s. percentages, these events are quite comparable to the following Bolling–Allerod warm event.

on the Celtic margin and which indicate supply of BIS-sourced IRD ahead of Laurentide Ice Sheet-sourced IRD (Scourse et al., 2000). Multi-proxy study of Porcupine Seabight core MD01-2461 indicates also significant warming in SST just prior to the precursor IRD discharges (Peck et al., 2004, submitted for publication). Warm water inflow to the margin at that time could have resulted in similar disintegration of the BIS. This melting would result in a significant freshwater flux which might perturb the convective overturning (Broecker et al., 1990), and therefore disrupt or disturb the thermohaline circulation (THC). This would then inhibit the northward flow of warm surface water in the Bay of Biscay, so causing a cooling; this is supported by the synchronous high percentages of *N. pachyderma* s. during this period (Fig. 12). The robustness of these interpretations might be questioned considering the current debate that exists about the role and efficacy of the ocean thermohaline circulation and the conveyor belt in climate changes (Raymo et al., 2004), especially the response of the North Atlantic Deep Water to meltwater pulses (e.g. Piotrowski et al., 2004). However, our work does not offer any data on deep water responses, only sea-surface changes and the regional pattern of the THC.

Such laminated facies also have direct analogues in the Labrador Sea (Hesse and Khodabakhsh, 1998) in that they are dominantly clayey but also contain coarse detrital grains. In the Bay of Biscay the latter were probably transported by ice-rafting sourced from the BIS (Fig. 1). However, according to Hesse and Khodabakhsh (1998), the fines are the result of plume downwelling charged with suspended matter which cascade to a level determined by buoyancy within the water column. This results in the combination of fines from turbid meltwater and coarse grains supplied by icebergs. These laminated facies, characterised by high sedimentation rate (ex: 460 cm/ka in the core MD95-2002), suggest seasonal periodicity in BIS melting. We envisage the following stages (Fig. 14):

In spring, insolation accentuates the evaporation of equatorial waters which intensifies the poleward heat transport. The margins of the BIS in contact with this warm water destabilise and calve icebergs, which at this latitude, melt almost immediately and release IRD. In parallel, the ice sheet and the surrounding glaciers melt partially and liberate, via the plume of the "Manche" palaeoriver and through the Irish Sea, large quantities of turbid meltwater. These dense turbid plumes cascade and supply the deep ocean with clayey material (Fig. 14). This process assemblage results in the clayey IRD-rich dark lamination.

In summer, high temperatures inhibit release of icebergs, and meltwater sedimentation alone results in argillaceous sedimentation. This explains the primarily argillaceous homogeneous deposit (light laminae) (Fig. 14).

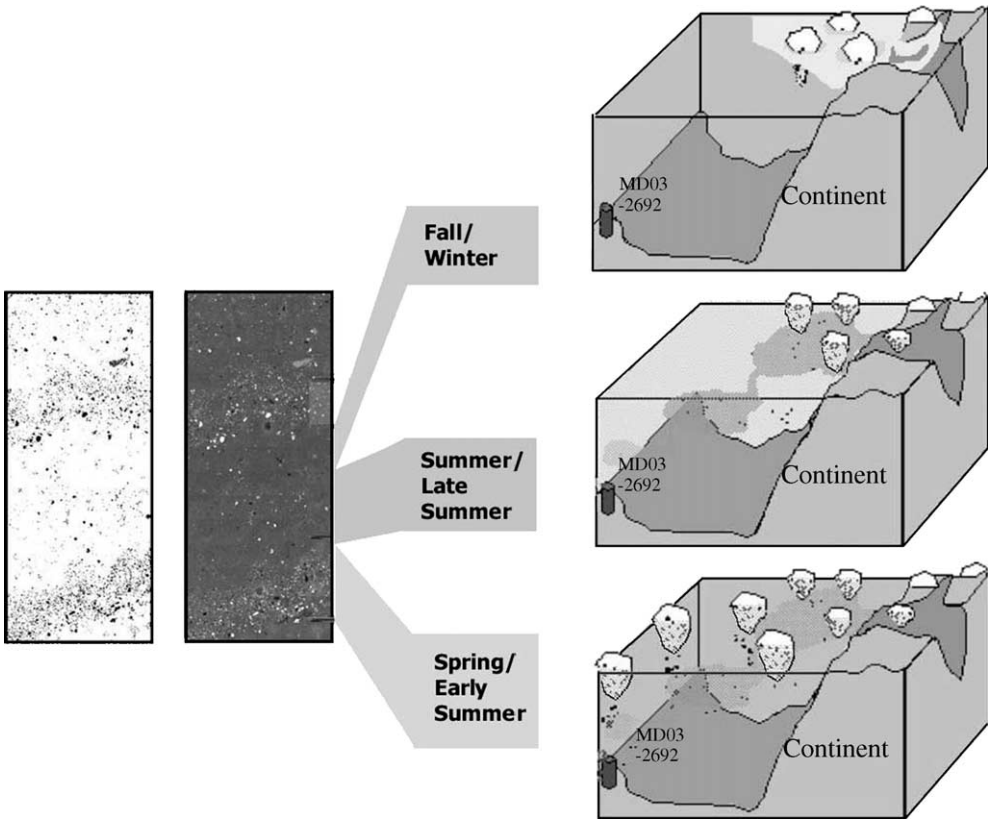

Fig. 14. Conceptual diagrams of the proposed model of laminated sediment deposition.

In winter, freezing temperatures generate sea-ice that inhibits iceberg production and melting. Residual argillaceous sedimentation takes place during this phase (Fig. 14).

5.2. MIS 6 (Fig. 15)

During MIS6, six Heinrich events have been observed (Fig. 15). We have identified and numbered them in comparison with previous studies from the North-East Atlantic (van Kreveld et al., 1996; Moreno et al., 2002). They are characterised by significant concentrations of coarse detrital IRD grains, relatively high values for magnetic susceptibility and large increases in percentages of the polar taxon *N. pachyderma* s.

The presence of laminated facies similar to those described in Termination I is noteworthy. However, these laminations occur well before Termination II: i.e. about 19 ka early. Previous studies (Locascio, 2003) have associated such facies with terminations. So, if these laminated facies are primarily due to climatic warming associated with the onset of interglacial stages, why do they occur so much earlier in MIS 6?

A study carried out by Schneider et al. (1999) on an equatorial core records an increase of alkenone SST 20 ka before the onset of the northern hemisphere deglaciation at the end of MIS 6 (Fig. 16). According to their long-term record, this phasing is specific only to Termination II. All other terminations record SST that is synchronous with global ice volume variations ($\delta^{18}O$). It is therefore possible that such a warming, occurring in the tropics at 151 ka and forced by eccentricity (Fig. 16), could have affected melting of the BIS. This event occurred 20 ka before the onset of the "real" northern hemisphere deglaciation, suggesting that the BIS was out of phase with other northern hemisphere ice sheets. The consequence of this conclusion is that these facies are not tied to terminations

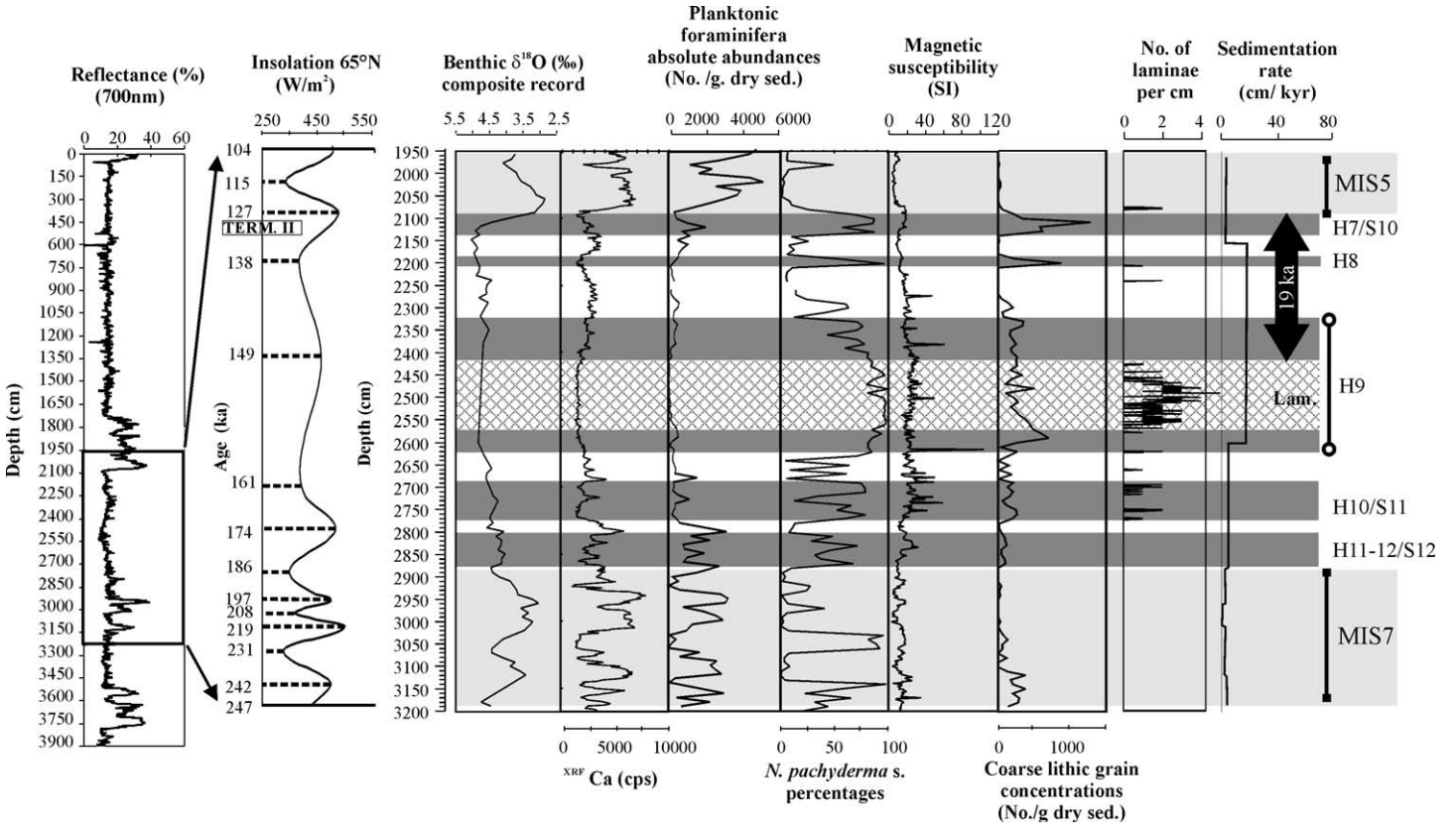

Fig. 15. Synthetic figure summarizing the various results obtained on the penultimate climatic cycle. Data are plotted along depth in the core to avoid graphic distortion. Some age pointers are localized on the 65°N July insolation curve for each inflexion point of this parameter. Termination II onset was positioned according to Sarnthein and Tiedemann (1990). Dark gray bars mark "Heinrich like events" after van Kreveld et al. (1996) and Moreno et al. (2002).

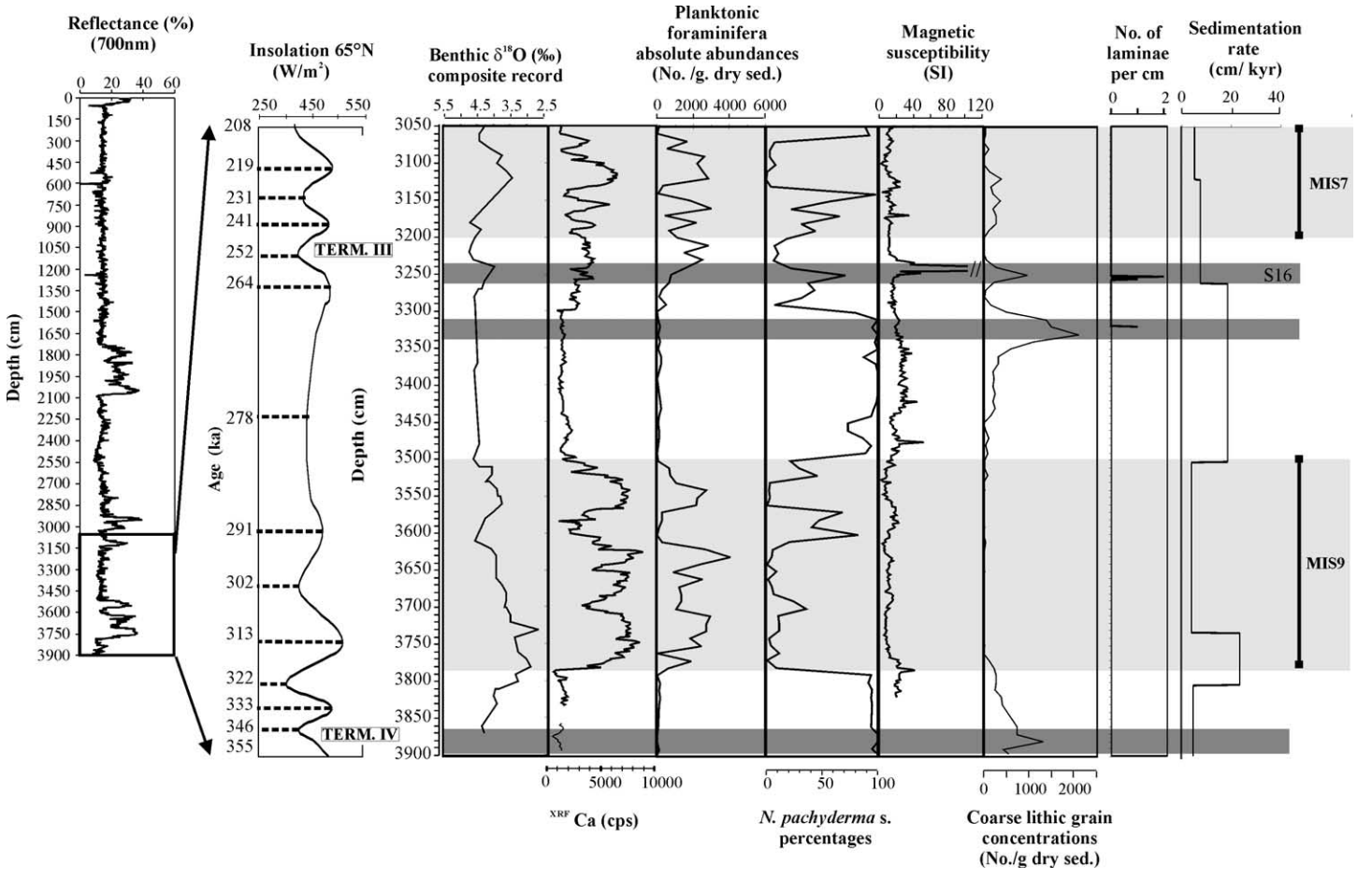

Fig. 16. Synthetic figure summarizing the various results obtained on the antepenultimate climatic cycle. Data are plotted along depth in the core to avoid graphic distortion. Some age pointers are localized on the 65°N July insolation curve for each inflexion point of this parameter. Termination III and IV onsets were positioned according to Sarnthein and Tiedemann (1990). Dark gray bars mark "Heinrich like events"; S16 after Moreno et al. (2002).

i.e. to global ice volume, but rather to the glacimarine conditions associated with rapid deglaciation of local ice sheets. These arguments imply early melting of the BIS in MIS 6, but additional studies are required to test this hypothesis.

5.3. MIS 8 (Fig. 16)

Similar Heinrich events are also observed during MIS 8. The youngest one identified could be S16, also identified by Moreno et al. (2002) on the Portuguese margin. It is called S16 and not HL16 because it has been established only on the basis of magnetic susceptibility. Our data confirm that the term "Heinrich like event" is appropriate since this level contains concentrations of coarse detrital IRD grains, as high as in HL4 (Fig. 12), high percentages of *N. pachyderma* s., and a large peak in magnetic susceptibility.

Termination III is not characterised by laminated facies in our core (Fig. 16). This questions the existence of a significant BIS at the end of MIS 8; interestingly, MIS 8 records of sea-level (Waelbroek et al., 2001; Sidall et al., 2003) imply smaller global ice volume for this stage (sea-level reaches −100 m, compared with −120 m during MIS 2 and 6). Assuming that the growth and decay of the BIS were in phase with patterns of global ice volume, then the BIS could have been small in extent or not present at all in MIS 8. This is consistent with Bowen (1999) who has been unable to find evidence in support of southern ice margin extension of the BIS during MIS 8. Other cores are obviously needed to definitively test this hypothesis.

5.4. Synthesis

Previous studies on the Celtic margin have highlighted the presence of laminated facies within last deglaciation sequences (Zaragosi et al., 2001; Locascio, 2003). High sedimentation rates recorded during these events suggest seasonal deposition. The presence of this specific facies, apparently linked here to BIS history, but also recorded elsewhere on glaciated margins during Termination I (Lekens et al., 2005), generates the hypothesis that such facies might be associated with earlier Terminations. The length of the record preserved in core MD03-2692 has enabled us to test this hypothesis. The significant results are:

1. At Termination I, the laminated facies constitutes a precursor to HL1 and is probably the result of a major disintegration event of the BIS. This event may have been stimulated by the warming following the LGM linked to increasing insolation at 65°N marking the onset of global deglaciation. According to a seasonal decay assumption, the counting of the laminae (a couplet [clear–dark]=1 yr) indicates that this sequence contains 91 yrs (91 dark laminae). However, the age model reconstituted suggests a duration of about 600 yrs. This difference is probably due to: (1) the resolution of the tie-points used for the dating which is insufficient to resolve such abrupt events, especially considering ventilation changes associated with meltwater events (e.g. Voelker et al., 1998; Waelbroek et al., 2001) and, (2) the relatively distal position of the core to the BIS (Fig. 1) which as a result probably recorded only the most intense phase of ice sheet collapses. The reduced sedimentation rates towards the Trevelyan escarpment (MD03-2692: 90 cm/ka during this event) compared with the Meriadzeck terrace (MD95-2002: 460 cm/ka) corroborate this last supposition.
2. Termination II does not contain laminated facies: instead these are found within MIS 6, 19000 yrs before the deglaciation. Based on our data and the rather few references relating to MIS 6 high-resolution studies, this does seem to be a rather unusual glacial stage. Schneider et al. (1999) identified an early warming in the tropics at 151 ka that could have forced BIS melting, generating the typical laminated facies. Assuming that this melting is also seasonal, lamination counts suggest that the intense phase of this event would have lasted 150 yrs.
3. Termination III contains no laminated sedimentary layers. This could indicate reduced magnitude or even the absence of the BIS during MIS 8 as suggested by Bowen (1999).

6. Conclusions

High-resolution study of core MD03-2692 has enabled palaeoenvironmental reconstruction of the

Bay of Biscay during the last 360 ka. The multi-proxy data highlight the direct influence of the decay of the BIS, which profoundly influenced the palaeoceanography in the Bay of Biscay. There are very few cores along the European margin, and especially in the Bay of Biscay, which permit the investigation of more than one climatic cycle. Core MD03-2692 contains a long record which enables us to reconstruct events before the start of the last climatic cycle. This has enabled comparison of the last three climatic cycles, focusing primarily on the glacial stages and deglaciation phases hitherto poorly documented in the area. All the investigated glacial stages (stages 2, 4, 6, 8 and 10) record abrupt events (i.e. "Heinrich" or "Heinrich like" events) characterized by the predominance of the polar foraminifera *N. pachyderma* s., testifying to very cold sea-surface conditions, and by peaks in magnetic susceptibility and coarse IRD. We have investigated the internal microfabrics of Heinrich layers for the first time.

The major point of comparison between the last three deglaciations is the presence or absence of laminated deposits. These are interpreted to be a consequence of seasonal melting of the BIS resulting in the cascading of turbid melting waters concurrent with the deposition of IRD during iceberg calving. The presence of these deposits is conditioned by two parameters: (1) *ice sheet extension*: only major glaciations permit extensive growth of the temperate BIS; (2) *solar forcing*: climatic warming is necessary to initiate ice sheet collapse.

Further work is necessary to test these hypotheses. Other long high-resolution proximal records are needed in order to compare the key periods of deglaciation, and to test if Terminations IV, V, VI, and beyond are characterized by laminated facies or not. Other present or past-glaciated margins (e.g. Weddell Sea, Voring Plateau, Labrador Sea) need also to be investigated: analogues should be explored to validate the environmental controls of laminae formation. This would help to constrain the seasonal cyclicity inherent in laminae couplet formation and therefore the duration of these events within BIS deglaciation.

Acknowledgements

Thanks are due to IPEV, the captain and the crew of the *Marion Dufresnes* and the scientific team of the SEDICAR cruise. We wish to thank Mr. Y. Balut for his assistance at sea and O. Ther, G. Chabaud, K. Charlier, L. Lavelle, D. P. Kennedy, B. Martin, D. Poirier and J. St Paul for laboratory assistance. XRF measurements were supported by the EU-project PALEOSTUDIES (Contract No.: HPRI-CT-2001-0124). Parts of the analyses conducted at the DGO were supported by the SHOM. This paper greatly benefits from the review of two anonymous reviewers and from D. J.W. Piper, the editor in Chief of Marine Geology. This is an U.M.R./ EPOC C.N.R.S. 5805 contribution No. 1564.

References

Auffret, G.A., Pujol, C., Baltzer, A., Bourillet, J.F., Müller, C., Tisot, J.P., 1996. Quaternary sedimentary regime on the Berthois Spur (Bay of Biscay). Geo Mar. Lett. 16, 76–84.

Auffret, G.A., Zaragosi, S., Dennielou, B., Cortijo, E., Van Rooij, D., Grousset, F., Pujol, C., Eynaud, F., Siegert, M., 2002. Terrigenous fluxes at the Celtic margin during the last glacial cycle. Mar. Geol. 188, 79–108.

Bard, E., 1998. Geochemical and geophysical implications of the radiocarbon calibration. Geochim. Cosmochim. Acta 62, 2025–2038.

Bard, E., 2002. Climate shock: abrupt changes over millennial time scales. Phys. Today 55, 32–39.

Bauch, D., Erlenkeuser, H., Winckler, G., Pavlova, G., Thiede, J., 2002. Carbon isotopes and habitat of polar planktic foraminifera in the Okhotsk Sea: the 'carbonate ion effect' under natural conditions. Mar. Micropaleontol. 45, 83–99.

Bénard, Y., 1996. Les techniques de fabrication des lames minces de sol. Cah. Techn. I.N.R.A. 37, 29–42.

Berger, A., Loutre, M.F., 1991. Insolation values for the climate of the last 10 million years. Quat. Sci. Rev. 10, 297–317.

Broecker, W.S., van Donk, J., 1970. Insolation changes, ice volumes, and the O18 record in deep sea cores. Rev. Geophys. Space Phys. 8, 169.

Broecker, W.S., Bond, G., Klas, M., 1990. A salt oscillator in the glacial Atlantic? 1. The concept. Paleoceanography 5 (4), 469–477.

Bond, G., Heinrich, H., Broecker, W., Labeyrie, L., McManus, J., Andrews, J., Huon, S., Jantschik, R., Clasen, S., Simet, C., Tedesco, C., Klas, M., Bonani, G., Ivy, S., 1992. Evidence for massive discharges of icebergs into the North Atlantic Ocean during the last glacial period. Nature 360, 246–249.

Boulton, G.S., Jones, A.S., Clayton, K.M., Kenning, M.J., 1977. A British ice-sheet model and patterns of glacial erosion and deposition in Britain. Br. Quat. Stud.: Recent, 231–246.

Bourillet, J.F., Lericolais, G., 2003. Morphology and seismic stratigraphy of the Manche paleoriver system, western approaches margin. In: Mienert, J., Weaver, P. (Eds.), European Margin

Sediment Dynamics: Side-Scan Sonar and Seismic Images. Springer, Berlin, pp. 229–232.
Bourillet, J.-F., Turon, J.-L., 2003. Rapport scientifique de la mission MD133/SEDICAR. OCE/2003/04. Les Rapports de Campagne à la MerIPEV, Brest. 150 pp.
Bourillet, J.F., Reynaud, J.Y., Baltzer, A., Zaragosi, S., 2003. The "Fleuve Manche": the sub-marine sedimentary features from the outer shelf to the deep-sea fans. J. Quat. Sci. 18, 261–282.
Bowen, D.Q., 1999. Only four major 100-ka glaciations during the Brunhes Chron? Int. J. Earth Sci. 88, 276–284.
Bowen, D.Q., Phillips, F.M., McCabe, A.M., Knutz, P.C., Sykes, G.A., 2002. New data for the last glacial maximum in Great Britain and Ireland. Quat. Sci. Rev. 21, 89–101.
Chapman, M.R., Shackleton, N.J., 1998. Millennial-scale fluctuations in North Atlantic heat flux during the last 150 000 years. Earth Planet. Sci. Lett. 159, 57–70.
Droz, L., Auffret, G., Savoye, B., Bourillet, J.F., 1999. L'Eventail profond de la marge Celtique: stratigraphie et évolution sédimentaire. C. R. Acad. Sci. Paris 328, 173–180.
Duplessy, J.-C., Shackleton, N.J., Matthews, R.K., Prell, W., Ruddiman, W.F., Caralp, M., Hendy, C.-H., 1983. ^{13}C record of benthic foraminifera in the last interglacial ocean: implications for the carbon cycle and the global deep water circulation. Quat. Res. 21, 225–243.
Eynaud, F., Turon, J.L., Sanchez-Goni, M.F., Gendreau, S., 2000. Dinoflagellate cyst evidence of 'Heinrich-like events' off Portugal during the marine isotopic stage 5. Mar. Micropaleontol. 40, 9–21.
Fairbanks, R.G., 1989. A 17,000-year glacio-eustatic sea level record: influence of glacial melting rates on the Younger Dryas event and deep-ocean circulation. Nature 342, 637–642.
Frew, R.D., Dennis, P.F., Karen, J.H., Michael, P.M., Steven, M.B., 2000. The oxygen isotope composition of water masses in the northern North Atlantic. Deep-Sea Res., Part 1, Oceanogr. Res. Pap. 47, 2265–2286.
Gibbard, P.L., 1988. The history of the great northwest European rivers during the past three million years. Philos. Trans. R. Soc. Lond. B 318, 559–602.
Gibbard, P.L., Lautridou, J.P., 2003. The quaternary history of the English channel: an introduction. J. Quat. Sci. 18, 195–199.
Grousset, F.E., Labeyrie, L.D., Sinko, J.A., Cremer, M., Bond, G., Duprat, J., Cortijo, E., Huon, S., 1993. Patterns of ice-rafted detritus in the glacial North Atlantic (40–55°N). Paleoceanography 8, 175–192.
Grousset, F., Pujol, C., Labeyrie, L., Auffret, G.A., Boelaert, A., 2000. Were the North Atlantic Heinrich events triggered by the behaviour of the European ice sheet? Geology 28, 123–126.
Heinrich, H., 1988. Origin and consequences of cyclic ice rafting in the northeast Atlantic Ocean during the past 130 000 years. Quat. Res. 29, 142–152.
Hesse, R., Khodabakhsh, S., 1998. Depositional facies of late Pleistocene Heinrich events in the Labrador Sea. Geology 26, 103–106.
Imbrie, J., Berger, A., Boyle, E.A., Clemens, S.C., Duffy, A., Howard, W.R., Kukla, G., Kutzbach, J., Martinson, D.G., McIntyre, A., Mix, A.C., Molfino, B., Morley, J.J., Peterson, L.C., Pisias, N.G., Prell, W.L., Raymo, M.E., Shackleton, N.J., Toggweiler, J.R., 1993. On the structure and origin of major glaciation cycles: 2. The 100,000 year cycle. Paleoceanography 8, 699–735.
Joussaume, S., 2000. Climat d'hier à demain. CEA/CNRS editions, Paris.
Knight, J., 2004. Devensian glacial events in the north of Ireland. Geol. J. 39, 403–417.
Larsonneur, C., Auffret, J.-P., Smith, A.-J., 1982. Carte des Paleo-Vallées et des Bancs de la Manche Orientale. BRGM editions. (1/500 000eme).
Lambeck, K., 1995. Late Devensian and Holocene shorelines of the British Isles and North Sea from models of glacio–hydro–isostatic rebound. J. Geol. Soc. 152, 437–448.
Lambeck, K., Yokoyama, Y., Purcell, T., 2002. Into and out of the last glacial maximum: sea-level change during oxygen isotope stages 3 and 2. Quat. Sci. Rev. 21, 343–360.
Le Suavé, R., Bourillet, J.-F., Coutelle, A., 2000. La Marge Nord du Golfe de Gascogne. Connaissances Générales et Apport des Nouvelles Synthèses de Données Multifaisceaux. Synthèse Bathymétrique et Imagerie Acoustique de la Zone Économique Exclusive Atlantique Nord-Est. IFREMER ed. 55 pp.
Lekens, W.A.H., Sejrup, H.P., Haflidason, H., Petersen, G.O., Hjelstuen, B., Knorr, G., 2005. Laminated sediments preceding Heinrich event 1 in the northern North Sea and southern Norwegian Sea: origin, processes and regional linkage. Mar. Geol. 216, 27–50.
Lericolais, G., 1997. Evolution Plio–Quaternaire du Fleuve Manche: Stratigraphie et Géomorphologie d'une Plateforme Continentale en Régime Périglaciaire. PhD thesis, Univ. Bordeaux I. 265 pp.
Lericolais, G., Auffret, J.-P., Bourillet, J.-F., 2003. The quaternary channel river: seismic stratigraphy of its palaeo-valleys and deeps. J. Quat. Sci. 18, 245–260.
Locascio M., 2003. La déglaciation Saalienne en Europe de l'Ouest: investigation très haute résolution et multiproxies d'une carotte de la Marge Irlandaise. Master thesis, Univ. Bordeaux I. 30 pp. (available online via the ASF website: http://www.sedimentologie.com).
Loutre, M.-F., Berger, A., 2003. Marine isotope stage 11 as an analogue for the present interglacial. Glob. Planet. Change 36, 209–217.
Manighetti, B., McCave, I.N., 1995. Depositional fluxes, paleoproductivity, and ice rafting in the NE Atlantic over the past 30 kyr. Paleoceanography 10, 579–592.
Martin, G.-B., Thorrold, S.-R., Jones, C.-M., 2004. Temperature and salinity effects on Sr incorporation in otoliths of larval spot (*Leiostomus xanthurus*). Can. J. Fish. Aquat. Sci. 61, 34–42.
Martinson, D.G., Pisias, N.G., Hays, J.D., Imbrie, J., Moore Jr., T.C., Shackleton, N.J., 1987. Age dating and the orbital theory of the ice ages: development of a high-resolution 0 to 300,000-year chronostratigraphy. Quat. Res. 27, 1–29.
Mc Cabe, A.-M., 1998. Striae at St. Mullin's Cave, County Kilkenny, southern Ireland: their origin and chronological significance. Geomorphology 23, 91–96.
Mc Cabe, A.M., Clark, P.U., 1998. Ice sheet variability around the North Atlantic Ocean during the last deglaciation. Nature 392, 373–377.

McIntyre, A., Ruddiman, W.F., Jantzen, R., 1972. Southward penetrations of the North Atlantic polar front: faunal and floral evidence of large-scale surface water mass movements over the last 225 kyr. Deep-Sea Res. 19, 61–77.

McManus, J.F., Bond, G.C., Broecker, W.S., Johnsen, S., Labeyrie, L., Higgins, S., 1994. High-resolution climate records from the North Atlantic during the last interglacial. Nature 371, 326–329.

Migeon, S., Weber, O., Faugeres, J.C., Saint-Paul, J., 1999. SCOPIX: a new imaging system for core analysis. Geo. Mar. Lett. 18, 251–255.

Mix, A.E., Bard, E., Schneider, R., 2001. Environmental processes of the ice age: land, ocean, glaciers (EPILOG). Quat. Sci. Rev. 20, 627–657.

Moreno, E., Thouveny, N., Delanghe, D., McCave, I.-N., Shackleton, N.-J., 2002. Climatic and oceanographic changes in the northeast Atlantic reflected by magnetic properties of sediments deposited on the Portuguese Margin during the last 340 ky. Earth Planet. Sci. Lett. 202, 465–480.

Paillard, D., Labeyrie, L., Yiou, P., 1993. Macintosh program performs time-series analysis. EOS Trans. AGU 77, 379.

Peck, V., Hall, I.R., Zahn, R., Elderfield, H., Grousset, F.E., Scourse, J.D., 2004. Sequencing ice–ocean–climate interaction in the NE Atlantic during the Last Glacial. 8th International Conference on Paleoceanography Biarritz, September 2004. Abstract volume 191.

Peck, V.L., Hall, I.R., Zahn, R., Elderfield, H., Grousset, F., Hemming, S., Scourse, J.D., submitted for publication. High resolution evidence for linkages between European ice sheet instability and Atlantic meridional overturning circulation changes. Earth and Planet. Sci. Lett.

Piotrowski, A.M., Goldstein, S.L., Hemming, S.R., Fairbanks, R.G., 2004. Intensification and variability of ocean thermohaline circulation through the last deglaciation. Earth Planet. Sci. Lett. 225, 205–220.

Raymo, M.E., Oppo, D.W., Flower, B.P., Hodell, D.A., McManus, J.F., Venz, K.A., Kleiven, K.F., McIntyre, K., 2004. Stability of North Atlantic water masses in face of pronounced climate variability during the Pleistocene. Paleoceanography 19, 1–13 (PA2008).

Richter, T.O., Lassen, S., van Weering, Tj.-C.-E., De Haas, H., 2001. Magnetic susceptibility patterns and provenance of ice-rafted material at Feni Drift, Rochall Trough: implications for the history of the British–Irish ice sheet. Mar. Geol. 173, 37–54.

Ruddiman, W.F., 1977. Late quaternary deposition of ice-rafted sand in the subpolar north Atlantic (lat 40° to 65° N). Geol. Soc. Amer. Bull. 88, 1813–1827.

Ruddiman, W.F., McIntyre, A., 1976. Northeast Atlantic paleoclimatic changes over the past 600 kyr. Geol. Soc. Amer. Mem. 145, 111–146.

Sarnthein, M., Tiedemann, R., 1990. Younger Dryas-style cooling events at glacial terminations I–VI at ODP site 658: associated benthic $\delta^{13}C$ anomalies constrain meltwater hypothesis. Paleoceanography 5, 1041–1055.

Scourse, J.D., 1991. Late Pleistocene stratigraphy and palaeobotany of the Isles of Sicily. Philos. Trans. R. Soc. Lond., B 334, 405–448.

Scourse, J.D., Furze, M.F.A., 2001. A critical review of the glaciomarine model for Irish Sea deglaciation: evidence from southern Britain, the Celtic shelf and adjacent continental slope. J. Quat. Sci. 16, 419–434.

Scourse, J.D., Austin, W.E.N., Bateman, R.M., Catt, J.A., Evans, C.D.R., Robinson, J.E., Young, J.R., 1990. Sedimentology and micropalaeontology of glacimarine sediments from the central and southwestern Celtic Sea. In: Dowdeswell, J.A., Scourse, J.D. (Eds.), Glacimarine Environments: Processes and Sediments, Special Publication of the Geological Society, vol. 53. The Geological Society, London, pp. 329–347.

Scourse, J.D., Hall, I.R., Mc Cave, I.-N., Young, J.-R., Sugdon, C., 2000. The origin of Heinrich layers: evidence from H2 for European precursor events. Earth Planet. Sci. Lett. 182, 187–195.

Schneider, R., Müller, P.-J., Acheson, R., 1999. Atlantic alkenone sea-surface temperature records, low versus mid latitudes and differences between hemispheres. In: Abrantes, F., Mix, A.C. (Eds.), Reconstructing Ocean History: A Window into the Future. Plenum, New-York, pp. 33–56.

Sidall, M., Rohling, E.-J., Almogi-Labin, A., Hemleben, C., Meischner, D., Schmelzer, I., Smeed, D.A., 2003. Sea-level fluctuations during the last glacial cycle. Nature 423, 853–858.

Stokes, C.R., Clark, C.D., 2001. Palaeo-ice streams. Quat. Sci. Rev. 20, 1437–1457.

Thinon, I., Fidalgo-Gonzalez, L., Rehault, J.-P., Olivet, J.-L., 2001. Pyrenean deformations in the Bay of Biscay. C. R. Acad. Sci. Ser. IIA, Earth Planet. Sci. 332 (9), 561–568.

Thouveny, N., Moreno, E., Delanghe, D., Candon, L., Lancelot, Y., Shackleton, N.J., 2000. Rock magnetic detection of distal ice-rafted debris: clue for the identification of Heinrich layers on the Portuguese margin. Earth Planet. Sci. Lett. 180, 61–75.

van Aken, H.M., 2000. The hydrography of the mid-latitude northeast Atlantic Ocean: II. The intermediate water masses. Deep-Sea Res., Part 1, Oceanogr. Res. Pap. 47, 789–824.

van Kreveld, S.A., Knappertsbusch, M., Ottens, J., Ganssen, G.-M., van Hinte, J.-E., 1996. Biogenic carbonate and ice-rafted debris (Heinrich layer) accumulation in deep-sea sediments from northeast Atlantic piston core. Mar. Geol. 131, 21–46.

van Weering, T.-C.-E., Nielsen, T., Kenyon, H., Akentieva, K., Kuijpers, A.H., 1998. Sediments and sedimentation at the NE Faeroe continental margin; contourites and large-scale sliding. Mar. Geol. 152, 159–176.

Verbitsky, M., Saltzman, B., 1995. A diagnostic analysis of Heinrich glacial surge. Paleoceanography 10, 59–65.

Vidal, L., Labeyrie, L., Cortijo, E., Arnold, M., Duplessy, J.C., Michel, E., Becqué, S., van Weering, T.-C.-E., 1997. Evidence for changes in the North Atlantic deep water linked to meltwater surges during the Heinrich events. Earth Planet. Sci. Lett. 146, 13–27.

Voelker, A.H.L., Sarnthein, M., Grootes, P.M., Erlenkeuser, H., Laj, C., Mazaud, A., Nadeau, M.J., Schleicher, M., 1998. Correlation of marine C-14 ages from the Nordic seas with the GISP2 isotope record: implications for C-14 calibration beyond 25 ka BP. Radiocarbon 40, 517–534.

Waelbroek, C., Duplessy, J.C., Michel, E., Labeyrie, L., Paillard, D., Duprat, J., 2001. The timing of the last deglaciation in North Atlantic climate records. Nature 412, 724–726.

Weber, O., Gonthier, E., Faugères, J.-C., 1991. Analyse granulométrique de sédiments fins marins: comparaison des résultats obtenus au Sedigraph et au Malvern. Bull. Inst. Géol. Bassin Aquitaine 50, 107–114.

Zaragosi, S., Auffret, G.A., Faugeres, J.C., Garlan, T., Pujol, C., Cortijo, E., 2000. Physiography and recent sediment distribution of the Celtic deep-sea fan, Bay of Biscay. Mar. Geol. 169, 207–237.

Zaragosi, S., Eynaud, F., Pujol, C., Auffret, G.A., Turon, J.L., Garlan, T., 2001. Initiation of European deglaciation as recorded in the northwestern Bay of Biscay slope environments (Meriadzek Terrace and Trevelyan Escarpment): a multi-proxy approach. Earth Planet. Sci. Lett. 188, 493–507.